Investigating Force Control Strategies for a Servo Actuator

18. januar 2018
Student MCE7-724
Kristian Øeby Jørgensen
Department of Energy Technology

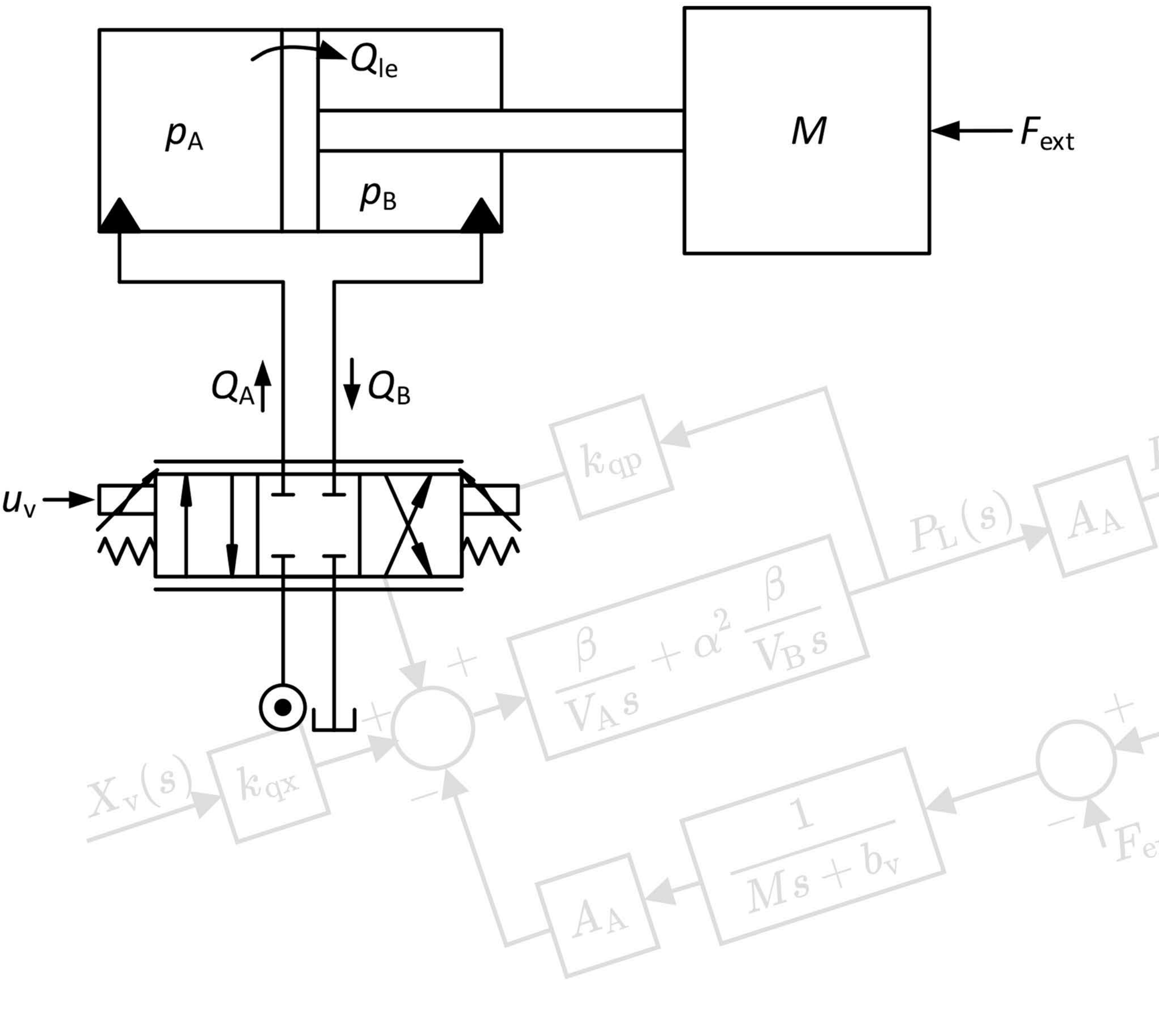

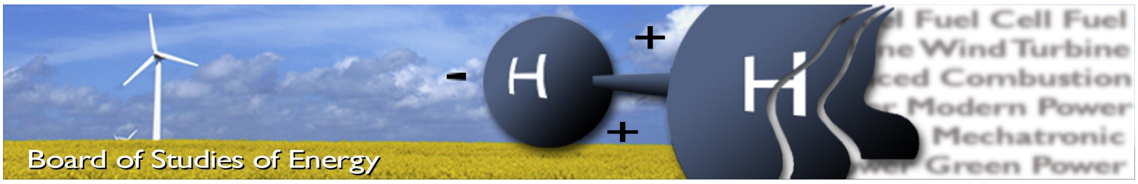

Title:	Investigating Force Control Strategies for a Servo Actuator
Semester:	7.
Semester theme:	Bachelor
Project period:	1. november 2017 - 18. january 2018
ECTS:	15
AAU supervisor:	Anders Hedegaard Hansen
R&D supervisor:	Søren Bruun
Student:	MCE7-724

This report investigates how a force controller to a servo actuator system consisting of an asymmetric cylinder and a symmetrical proportional valve may be designed. A non linear model of the system is derived and validated by comparing the simulated behaviour to the actual system behaviour. Using linear control theory, a PI controller is designed achieving satisfactory force tracking performance when given a sinusoidal force reference. To improve the controller, it is extended by employing a valve compensator. Best flow estimation performance is found when compensating with respect to one chamber pressure instead of both chamber pressures. The error was reduced when employing the compensator, and similar behaviour was achieved when lowering the supply pressure using a compensator while the error was increased without a compensator. It was found that the valve signal or force reference may be used to govern the compensator provided that the valve dynamic is sufficiently fast.
Similar force tracking performance is achieved when using a valve matched to the cylinder. The chamber pressure gradients are seen to be smoother, and a lower supply pressure is required.

Kristian Øeby Jørgensen

Pages, total:	71 pages
Appendix:	1
Supplements:	ZIP file

By accepting the request from the fellow student who uploads the study group´s project report in Digital Exam System, you confirm that all group members have participated in the project work, and thereby all members are collectively liable for the contents of the report. Furthermore, all group members confirm that the report does not include plagiarism.

Resume

Kraftstyring af hydrauliske cylindere benyttes i testbænke til at påføre testemner specifikke lastkrafter, men emnet er ikke ligeså bearbejdet som eksempelvis hastigheds- og positionsstyring. Kraftstyringen kan eksempelvis realiseres ved hjælp af en simpel linear regulator, som kan udvides ved at implementere en ventilkompensator. Forskellige regulatorformuleringer kan benyttes, og projektets problemformulering lyder:

"Hvordan kan en kraftregulator designes til at styre kraften i et hydraulisk servoaktuator system, og er det muligt at forbedre kraftregulatoren ved at implementere en ventilkompensator?"

En ulineær matematisk model formuleres for servoaktuator systemet. Modellen valideres ved at give ventilen et stepinput i et faktisk hydraulisk servoaktuator system og herefter benytte det målte stepinput, forsyningstryk og lastkraft som input i modellen. Kammertryk, stempelposition og -hastighed sammenlignes for systemet og modellen, og det konkluderes, at modellen emulerer det faktiske system tilstrækkeligt på trods af nogen afvigelse, som konkluderes at skyldes et offset på ventilen.

Modellen lineariseres, og på baggrund af en frekvensresponsalanyse af systemet vurderes det, at ventildynamikken bør inkluderes i den lineære model. En PI regulator designes på baggrund af den lineære model og viser tilfredsstillende performance, når en sinusformet kraftreference gives, dog med en gennemsnitlig fejl på 4.4 %.

En ventilkompensator designes til at udkompensere ventilforstærkningen med det formål at anvende viden om ventilen til at bestemme en ventiludstyring ud fra et ønsket flow. En PI regulator designes til at styre flowet ind og ud af stempelside-kammeret, og den gennemsnitlige fejl reduceres til 1.8 %. Det understreges, at denne forbedring kan skyldes, at flowregulatoren er designet en anelse mere aggresivt end den oprindelige PI regulator. En væsentlig forbedring med flowregulatoren og kompensatoren ses, da forsyningstrykket reduceres, og fejlen øges med 3 %, mens fejlen øges med 146 % med den oprindelige PI regulator. Den bedste estimering af flowet opnås, når der kompenseres ud fra et enkelt kammertryk fremfor begge kammertryk. Det konkluderes, at ventilsignalet kan bruges til at styre kompensatoren, hvis ventildynamikken er tilpas hurtig relativt til systemet.

Tilsvarende regulatorperformance opnås, når den symmetriske ventil udskiftes med en ventil, der matcher aktuatoren. Derudover opnås pænere trykgradienter, og det nødvendige forsyningstryk reduceres med 14 %.

Preface

This project is made by student MCE7-724 in collaboration with the company R&D A/S, during the 7th semester at the Department of Energy Technology, Aalborg University. The duration of the project spans from the 1st of November 2017 to the 18th of january 2018.

The preconditions for reading this report is an understanding of mechanical physics and control theory.

Reading guide

This report is divided into chapters, sections, subsections and subsubsections marked as follows:

First chapter: **1**

First section: **-.1**

First subsection: **-.-.1**

Subsubsection: **Bold**

All figures and selected tables include dedicated labels and captions that provide descriptions of each figure and selected tables. For instance, the first figure in Chapter 3 has the label 3.1. The tables that are part of the nomenclature are not labelled.

Nomenclatures describing variables used in equations will be placed after each set of equations with a symbol, a description and a unit. The variables will also be placed on a separate nomenclature list at the beginning of this report. Followed by the nomenclature for variables, there will also be a list of all the abbreviations used. When an abbreviation is first introduced in the text, it will be written in full followed by the abbreviation.

References are made according to the Harvard method and are labelled in the text as follows: [Name, Year]. If the name was not available, a website will be referred to instead. The references refer to the bibliography at the end of the report, where books are put with author, title, year and if possible publisher and ISBN. Web pages are put with author, title, URL, year and the date it was accessed during the project.

References are either placed at the end of a sentence or at the end of each paragraph. Appendixes are presented at the end of the report and listed as A, B, C etc.

The software MATLAB®R2017b and Simulink® are used for modelling, simulation and graphical data presentation.

A ZIP file containing MATLAB scripts, Simulink models, Datasheets, relevant literature and experimental data is attached.

Nomenclature

Symbol	Description	Unit
A	Area	m^2
β	Bulk modulus	Pa
ζ	damping	–
C_{d}	Discharge coefficient	–
f	Frequency	Hz
F	Force	N
k_{i}	Integral gain	–
k_{p}	Proportional gain	–
M	Mass	kg
p	Pressure	Pa
ρ	Density	kg/m^3
Q	Flow	m^3/s
s	Laplace operator	–
u_{v}	Valve signal	–
V	Volume	m^3
ω_{n}	Natural frequency	rad/s
x	Displacement	m

Transfer function	Description
$G_{\mathrm{v}}(s)$	Valve signal to spool position
$G_{\mathrm{Fx}}(s)$	Valve spool position to load force
$G_{\mathrm{Fu}}(s)$	Valve signal to load force
$G_{\mathrm{c}}(s)$	Force error to valve signal (Valve controller)
$G_{\mathrm{Fq}}(s)$	Piston side flow to load force
$G_{\mathrm{Fqref}}(s)$	Piston side reference flow to load force
$G_{\mathrm{cq}}(s)$	Force error to reference flow (Flow controller)

Table of Contents

Resume v

Preface vii

Nomenclature ix

Chapter 1 Introduction 1

Chapter 2 System Description 3

Chapter 3 Problem Statement 5
3.1 Problem Solution Strategy 5

Chapter 4 Modelling 7
4.1 Nonlinear Model 7
4.1.1 Hydraulic Model 8
4.1.2 Mechanical Model 11
4.1.3 Model Structure 14
4.1.4 Model Validation 14
4.2 Reduced Order Model 17
4.3 Linear Model 20

Chapter 5 Control Design 23
5.1 Force Controller 23
5.1.1 System Transfer Function 23
5.1.2 Frequency Response Analysis 25
5.1.3 Validation of Linear Model 28
5.1.4 Controller Design 30
5.1.5 Controller Performance in Non Linear Model 31

Chapter 6 Compensator Design 33
6.1 Valve Compensator 33
6.1.1 Load Pressure Compensating 34
6.2 Frequency Response Analysis 34
6.2.1 Flow Controller Design 36
6.3 Controller Performance in Non Linear Model 37
6.3.1 Comparison of Controller Performance 38
6.3.2 Robustness of Compensator 41
6.3.3 Compensating with Limited Feedback 43

Chapter 7 Matching Valve to Actuator Analysis 47
7.1 Matching Valve to Actuator Ratio 47

7.2 Controller Performance using a Matched Valve 48

Chapter 8 Force Control Design Considerations 51

Chapter 9 Conclusion 53

Chapter 10 Reflection 55

Bibliography 57

Appendix A System Parameters 59

Introduction 1

The company R&D A/S designs custom test benches for testing heavy duty equipment in industries such as wind, aerial, oil and gas among others. The purpose of the test benches is to apply specified load forces to the test objects which is achieved using hydraulic actuated systems. To apply desired load forces, high precision load control is required of these hydraulic actuators.

An example of one of these test benches is the Highly Accelerated Life Time (HALT) test bench for Lindoe Offshore Renewables Center (LORC) which is a recent project developed by R&D A/S as seen in Figure 1.1. The test bench serves to test the life time of complete nacelles by applying forces equivalent to those exerted on the nacelle by the wind but in a highly accelerated time horisont as indicated by the name.

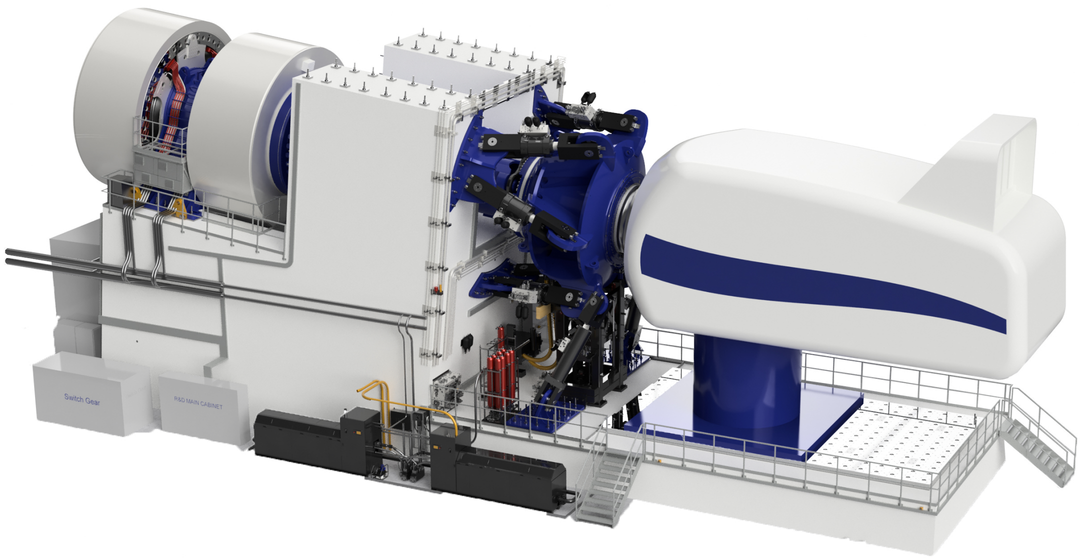

Figure 1.1. Highly Accelerated Life Time test bench at Lindoe Offshore Renewables Center.

The drive train is driven by two electrical motors, more specifically two direct drives. Additionally a test load unit actuated by nine hydraulic actuators delivers the forces on the main shaft usually exerted by the wind turbine blades as seen in the figure.

Different strategies are currently used at R&D A/S for controlling the servo valves of the actuators for implementing the force control. However, investigation of when different strategies should be applied has not been performed. Most available state of the art consider position and velocity control, leaving force control as a less investigated subject which will be the initial point of interest in this report.

System Description 2

The hydraulic actuation system on the HALT test bench consists of nine hydraulic actuators. Common for these are that they are asymmetrically constructed and controlled by a proportional servo valve. The subject of force control strategy is therefore in this report investigated with respect to a simple hydraulic system, consisting of a single asymmetric actuator controlled by a proportional servo valve. Such a configuration is often referred to as a servo actuator system, and one can be seen in Figure 2.1. The test benches constructed by R&D A/S are built for testing heavy equipment resulting in the load usually being very stiff and of high inertia. From this it is assumed that the load may be modelled as a mass, spring, damper system as seen in the figure.

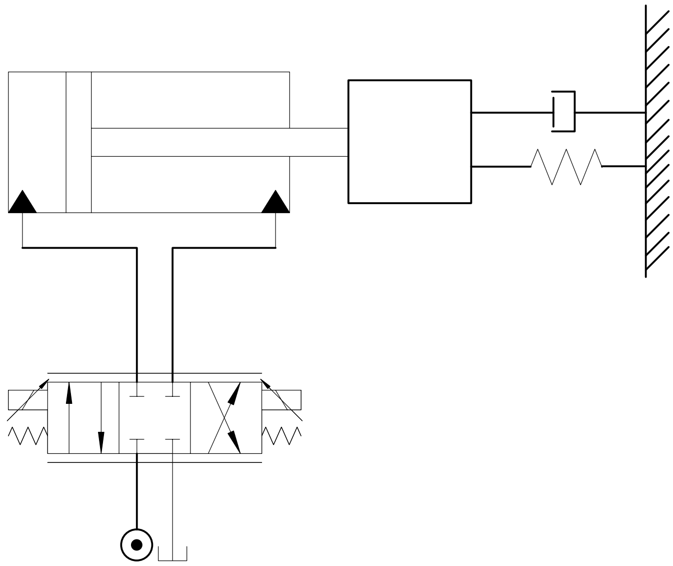

Figure 2.1. Hydraulic servo actuator system with a mass, spring, damper system as load.

At the test facility at Aalborg University a test bench is available meant for friction force estimation in hydraulic cylinders. The test setup consists of two asymmetric hydraulic actuators connected by a mass as seen in Figure 2.2. The cylinder to the right is usually considered as the main cylinder, whereas the left cylinder is considered the load. The pressure in the chambers of the main cylinder are controlled independently by two proportional valves while the load cylinder pressures are controlled by a single proportional valve. The servo actuator system desired for investigation as defined in Figure 2.1 may thereby be constructed by controlling the load cylinder with the single servo valve as indicated by the dashed line in Figure 2.2. Furthermore the mass and main cylinder may represent a stiff and high inertia load as suggested. By considering this system it is possible to construct a model which may afterwards be validated by comparing it to the test system.

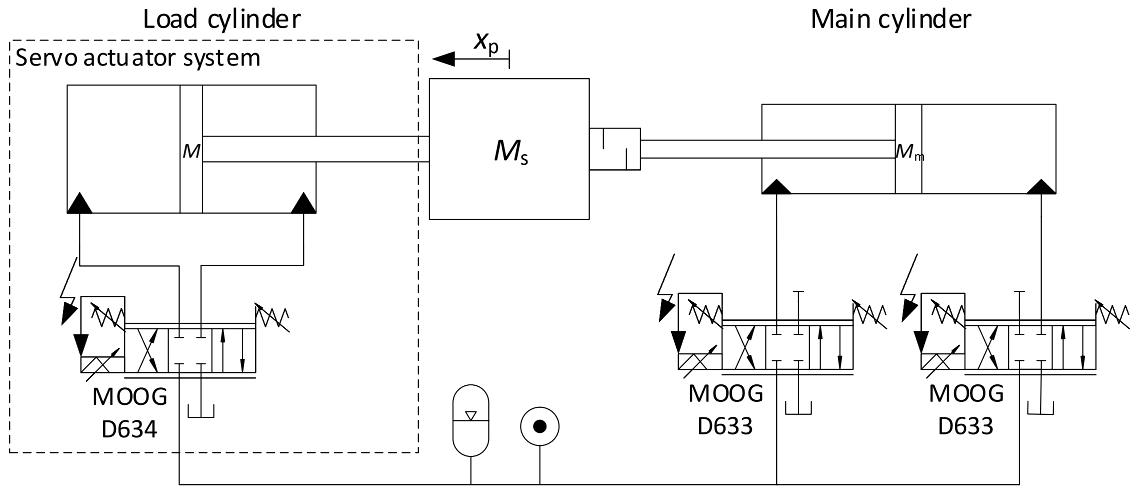

Figure 2.2. Hydraulic diagram of the back-to-back cylinder test bench.

Note that a force transducer, more specifically a load cell, measures the force between the main cylinder and the sliding mass. The measured system variables are listed in Table 2.1. System parameters are listed in Appendix A.

Variable	description
x_p	Piston position
$\dot{x}_\mathrm{p}$	Piston velocity
u_v	Valve signal
p_A	Piston side pressure
p_B	Rod side pressure
p_S	Supply pressure
F_cell	Force acting from main cylinder

Table 2.1. Measured system variables.

Figure 2.3 shows a picture of the test setup with the two hydraulic actuators combined by the sliding mass.

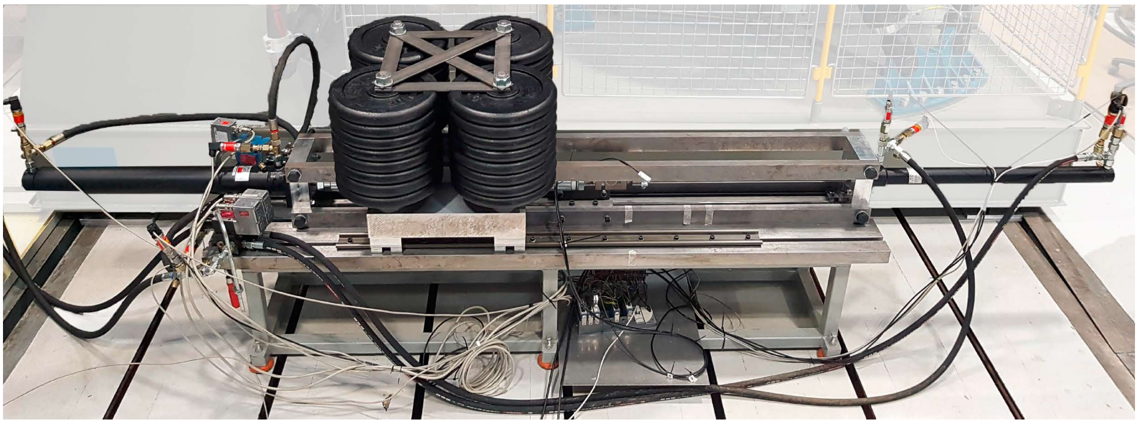

Figure 2.3. Back-to-back cylinder test bench at Aalborg University test facility.

3 Problem Statement

Based upon the point of interest stated in the introduction and the system described in the previous chapter, the problem statement is formulated as

"How may a force controller be designed for controlling the force in a hydraulic servo actuator system, and is it possible to improve the controller performance by employing a valve compensator?"

3.1 Problem Solution Strategy

To answer the problem statement the following solution strategy is developed:

1. Formulate a mathematical model describing the dynamics of the hydraulic servo actuator system.

- Derive a model describing the actuator and the valve.
- Validate the model by comparing it to the test system so that the model sufficiently depicts the system behaviour.
- Linearise the model so that linear control theory may be applied.
- Verify that the linear model behaviour depicts the nonlinear model to an acceptable degree.

2. Design different force controllers to the system.

- Formulate the linear model in the Laplace domain and derive a transfer function for the piston force system so a frequency analysis may be conducted.
- Design a force controller based on the analysis of the linear model and investigate its performance.
- Implement a valve compensator and investigate the impact it has on the control.
- Investigate how different formulation of the valve compensator influence the controller performance.
- Investigate the controller performance when using a valve matched to the cylinder.

3. Discussion of the performance of the derived force controllers and general considerations concerning the force controllers.

- Discussion of when different force controllers should be employed.
- General considerations about the designed force controllers.

Modelling 4

In this chapter a non linear system model is developed. To simplify system analysis a reduced order model is derived. Finally the reduced order model is linearised.

4.1 Nonlinear Model

The system with the asymmetric cylinder controlled with a proportional servo valve is seen in Figure 4.1. As seen in the figure the sliding mass has been included in the system. As the force transducer is placed between the main cylinder and the sliding mass it will be possible to validate the model. Due to uncertainty of the load characteristics the external force acting on the cylinder F_{ext} is kept as an input. By this it is possible to adjust the force in the model since it will be a system input rather than a part of the system. Note that the notation used in the setup described in Chapter 2 is retained. The piston position will thereby be zero as the piston is in the middle position and become positive as it moves to the left as indicated by the figure. This makes possible for an easy comparison with logged and normalised data from the laboratory setup.

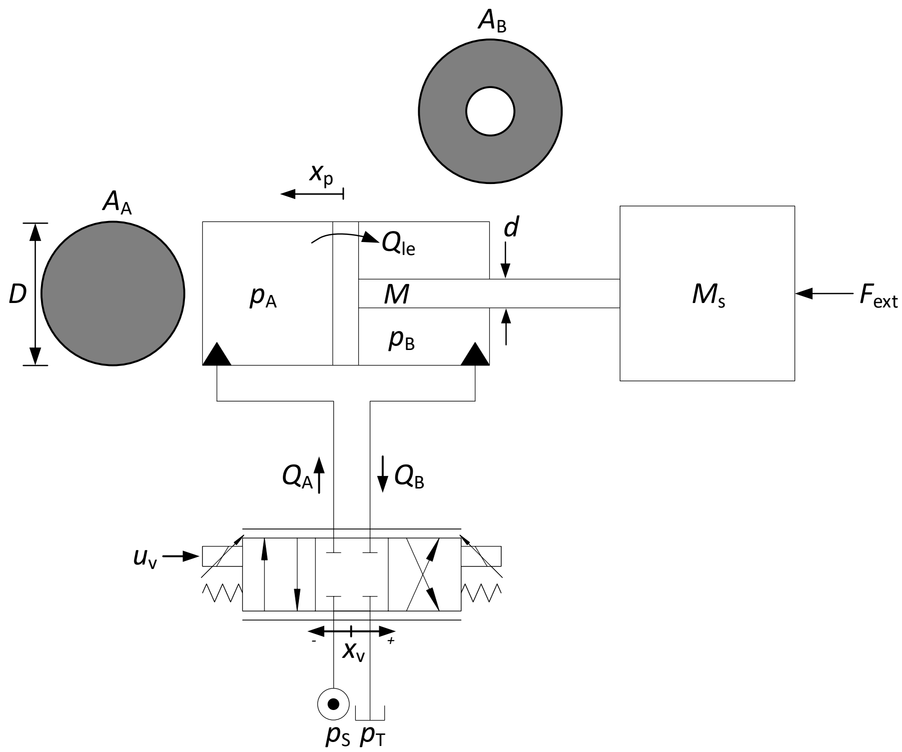

Figure 4.1. Diagram of the servo actuator system with system variables defined.

4.1.1 Hydraulic Model

A model of the system is now formulated in the time domain. The model is developed from a control volume approach where multiple fluid parameters, such as pressure, density, stiffness and temperature, are said to be equal in some defined volumes. This modelling approach is often refered to as lumped parameter modelling. There are two control volumes in the system, one for each cylinder chamber. The valve is installed close to the cylinder and it is assumed that the connections are rigid thereby assuming that hose volumes are constant. The control volumes are both bounded by the piston and the valve. The continuity equation is used to describe the control volumes and is seen in Equation 4.1.

$$Q_{\mathrm{in}} - Q_{\mathrm{out}} = \dot{V} + \frac{V}{\beta}\dot{p} \tag{4.1}$$

The continuity equations formulated for the control volumes are seen in Equations 4.2 and 4.3.

$$Q_{\mathrm{A}} - Q_{\mathrm{le}} = -\dot{x}_{\mathrm{p}} A_{\mathrm{A}} + \frac{V_{\mathrm{A0}} - x_{\mathrm{p}} A_{\mathrm{A}}}{\beta(p_{\mathrm{A}})}\dot{p}_{\mathrm{A}} \tag{4.2}$$

$$Q_{\mathrm{le}} - Q_{\mathrm{B}} = \dot{x}_{\mathrm{p}} A_{\mathrm{B}} + \frac{V_{\mathrm{B0}} + x_{\mathrm{p}} A_{\mathrm{B}}}{\beta(p_{\mathrm{B}})}\dot{p}_{\mathrm{B}} \tag{4.3}$$

Flow through a valve can generally be described by the orifice equation 4.4.

$$Q = C_{\mathrm{d}} A_{\mathrm{d}}(x_{\mathrm{v}})\sqrt{\frac{2}{\rho}\Delta p} \tag{4.4}$$

As can be seen the orifice equation contains multiple parameters related to the valve geometry which are determined numerically. However the datasheet for the valve MOOG D634 accounts for these valve proporties and lets the flow through the valve be described by Equation 4.5 at constant valve spool position. [MOOG, 2009]

$$Q = Q_{\mathrm{N}}\sqrt{\frac{\Delta p}{\Delta p_{\mathrm{N}}}} \tag{4.5}$$

with

Q_{N}	Nominal flow	100 l/min
Δp_{N}	Nominal pressure drop	35 bar
Δp	Actual pressure drop	- bar

Furthermore it can be seen from the datasheet that the valve is constructed so that the flow through the valve is proportional to the command signal for both positive and negative valve spool position as seen in Figure 4.2.

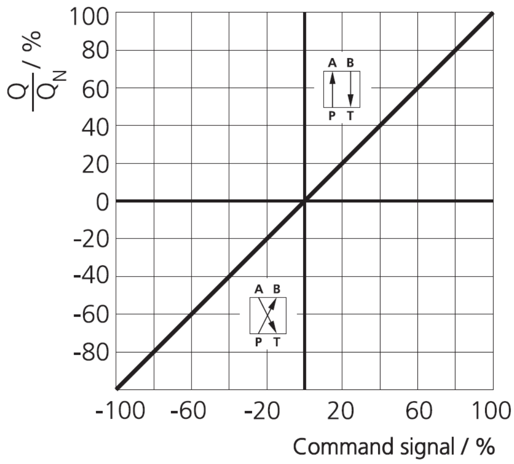

Figure 4.2. Flow characteristic for the servo valve MOOG D634. [MOOG, 2009]

This property allows for a rewriting of the flow expression which can then be expressed as a function of valve spool position as seen in Equation 4.6 and further reduced to Equation 4.7.

$$Q = Q_{\mathrm{N}} x_{\mathrm{v}} \sqrt{\frac{\Delta p}{\Delta p_{\mathrm{N}}}} \tag{4.6}$$

$$Q = \underbrace{\frac{Q_{\mathrm{N}}}{\sqrt{\Delta p_{\mathrm{N}}}}}_{k_{\mathrm{v}}} x_{\mathrm{v}} \sqrt{\Delta p} \tag{4.7}$$

The flow through the valve is then described by equations 4.8 and 4.9. If any leakage flow occur between the chambers it is assumed to occur in very small gaps why the flow can be assumed to be laminar and described proportional to the pressure difference as seen in Equation 4.10. It is assumed that no oil is leaked to the surroundings.

$$\begin{aligned} Q_{\mathrm{A}} = {} & k_{\mathrm{vA}} x_{\mathrm{v}} \sqrt{|p_{\mathrm{S}} - p_{\mathrm{A}}|} \mathrm{sgn}(p_{\mathrm{S}} - p_{\mathrm{A}})(x_{\mathrm{v}} \geq 0) \\ & + k_{\mathrm{vA}} x_{\mathrm{v}} \sqrt{|p_{\mathrm{A}} - p_{\mathrm{T}}|} \mathrm{sgn}(p_{\mathrm{A}} - p_{\mathrm{T}})(x_{\mathrm{v}} < 0) \end{aligned} \tag{4.8}$$

$$\begin{aligned} Q_{\mathrm{B}} = {} & k_{\mathrm{vB}} x_{\mathrm{v}} \sqrt{|p_{\mathrm{B}} - p_{\mathrm{T}}|} \mathrm{sgn}(p_{\mathrm{B}} - p_{\mathrm{T}})(x_{\mathrm{v}} \geq 0) \\ & + k_{\mathrm{vB}} x_{\mathrm{v}} \sqrt{|p_{\mathrm{S}} - p_{\mathrm{B}}|} \mathrm{sgn}(p_{\mathrm{S}} - p_{\mathrm{B}})(x_{\mathrm{v}} < 0) \end{aligned} \tag{4.9}$$

$$Q_{\mathrm{le}} = C_{\mathrm{le}}(p_{\mathrm{A}} - p_{\mathrm{B}}) \tag{4.10}$$

Note that for the valve MOOG D634 the valve constant for the chamber flows are equal, that is $k_{\mathrm{vA}} = k_{\mathrm{vB}} = k_{\mathrm{v}}$. The reason for distinguishing between the valve constant for the flow to the two chambers is that changing these may be desired to investigate the system behaviour with a proportional valve with a matched valve spool to actuator ratio.

Valve Dynamic

The servo valve does not operate instantaneously due to the acceleration of the valve spool mass in the oil. The frequency response and the step response for the valve is given in the datasheet MOOG [2009] and can be seen in Figure 4.3 and Figure 4.4, respectively.

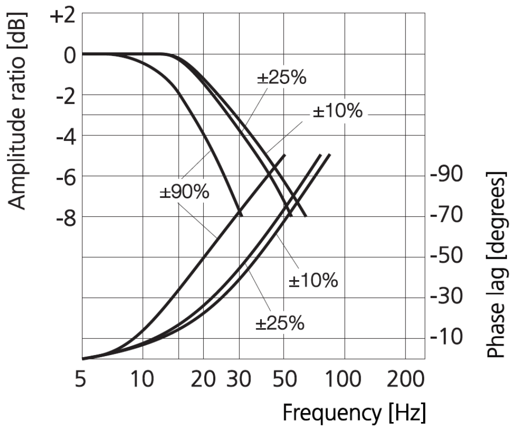

Figure 4.3. Frequency response of the servo valve MOOG D634. [MOOG, 2009]

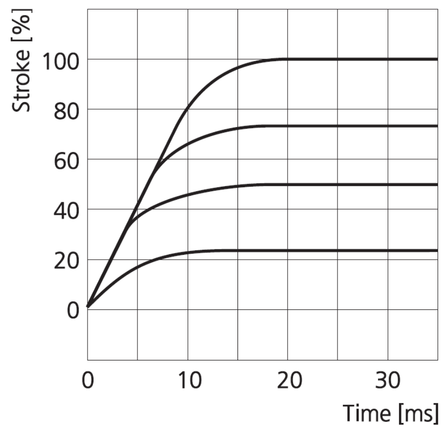

Figure 4.4. Step response of the servo valve MOOG D634. [MOOG, 2009]

The frequency response is seen to be slower for larger valve openings due to the limitation of available power to move the valve spool. The valve is modelled by approximating the frequency response as a second order transfer function for a valve opening of 10 %. To compensate for the slower frequency response at larger valve openings a slew rate limiter is implemented to limit the spool velocity to the slope seen from the step response of the valve. The second order transfer function is found by fitting it to chosen points such as the break away frequency from the frequency response at 10 % valve opening where it is desired to match both the magnitude and the phase as seen in Figure 4.5.

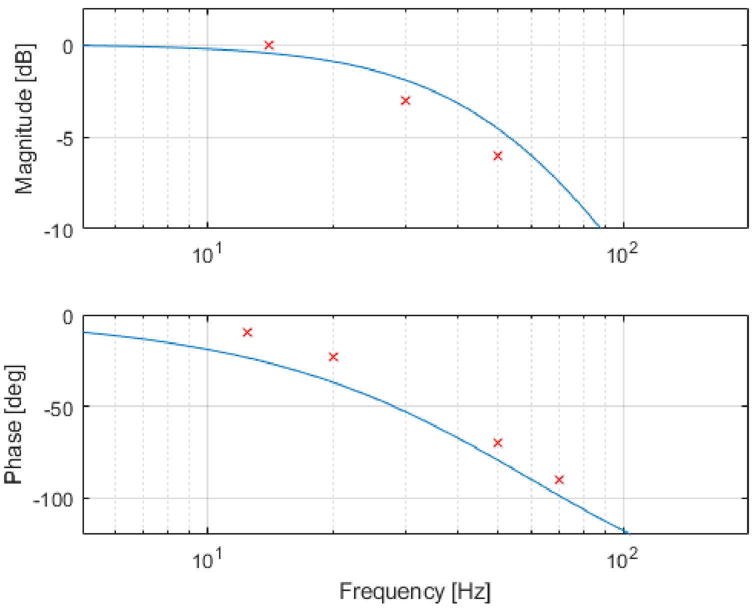

Figure 4.5. Second order approximation of the valve spool dynamic.

The valve is controlled by a voltage input ranging between $\pm 10V$ but the signal will be normalised when modelling the valve and the DC gain is thereby 1. The dynamic of the valve spool movement is thereby modelled as a second order transfer function from valve signal $U_{\mathrm{v}}(s)$ to spool movement $X_{\mathrm{v}}(s)$ as seen in Equation 4.11 with a slew rate limiter with the parameters listed in Table 4.1.

$$G_{\mathrm{v}}(s) = \frac{X_{\mathrm{v}}(s)}{U_{\mathrm{v}}(s)} = \frac{\omega_{\mathrm{v}}^2}{s^2 + 2\zeta_{\mathrm{v}}\omega_{\mathrm{v}}s + \omega_{\mathrm{v}}^2} \tag{4.11}$$

Parameter	Value	Unit
ω_{v}	377	rad/s
ζ_{v}	1	-
$\dot{x}_{\mathrm{v,max}}$	± 80	1/s

Table 4.1. Valve parameters derived from datasheet.

4.1.2 Mechanical Model

To model the movement of the piston it it necessary to locate the forces acting on it. A diagram of the cylinder illustrating the acting forces is seen in Figure 4.6.

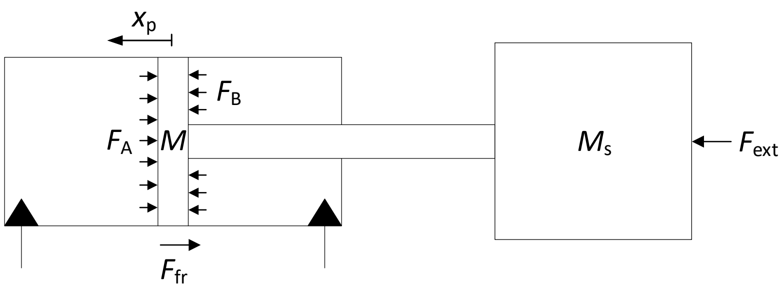

Figure 4.6. Forces acting on the piston.

The hydraulic forces are described as the product of the pressure in the chamber and the piston area it is working on. The piston movement can be described by formulating newtons second law for the piston as seen in Equation 4.12.

$$\ddot{x}_{\mathrm{p}} M_{\mathrm{tot}} = p_{\mathrm{B}} A_{\mathrm{B}} - p_{\mathrm{A}} A_{\mathrm{A}} - F_{\mathrm{fr}} + F_{\mathrm{ext}} \tag{4.12}$$

Where M_{tot} is the total moving mass of the system. F_{fr} is the friction force opposing the movement of the piston and F_{ext} is an external force acting on the cylinder. These forces will be described in the following, respectively.

Friction Model

By assuming the friction in the cylinder consists of a stribeck friction, a viscous friction and a coulomb friction the friction in the cylinder can be described by the Stribeck friction model seen in Equation 4.13. [Andersson et al., 2005]

$$F_{\text{fr}}(\dot{x}_{\text{p}}) = \text{sgn}(\dot{x}_{\text{p}})\left(b_{\text{v}}|\dot{x}_{\text{p}}| + F_{\text{c}} + (F_{\text{s}} - F_{\text{c}})e^{-\frac{|\dot{x}_{\text{p}}|}{c_{\text{s}}}}\right) \tag{4.13}$$

Where

b_{v}	Viscous friction parameter
c_{s}	Stribeck parameter
F_{c}	Constant coulomb friction
F_{s}	Maximum static friction

The Stribeck friction model can cause numerical problems when the sliding direction is changed due to discontinuity in the sign function at $\dot{x}_{\text{p}} = 0$. This is countered by reformulating the Stribeck friction model by introducing a hyperbolic tangent function as seen in Equation 4.14.

$$F_{\text{fr}}(\dot{x}_{\text{p}}) = \tanh\left(\frac{\dot{x}_{\text{p}}}{\gamma}\right)\left(F_{\text{c}} + (F_{\text{s}} - F_{\text{c}})e^{-\frac{|\dot{x}_{\text{p}}|}{c_{\text{s}}}}\right) + b_{\text{v}}\dot{x}_{\text{p}} \tag{4.14}$$

Where the γ-value determines the slope of the transient area of the coulomb friction. The different friction components as well as the friction model is plotted as function of piston velocity in Figure 4.7. The friction force parameters are fitted when the model is validated to achieve the correct magnitude of the friction force in Chapter 4.

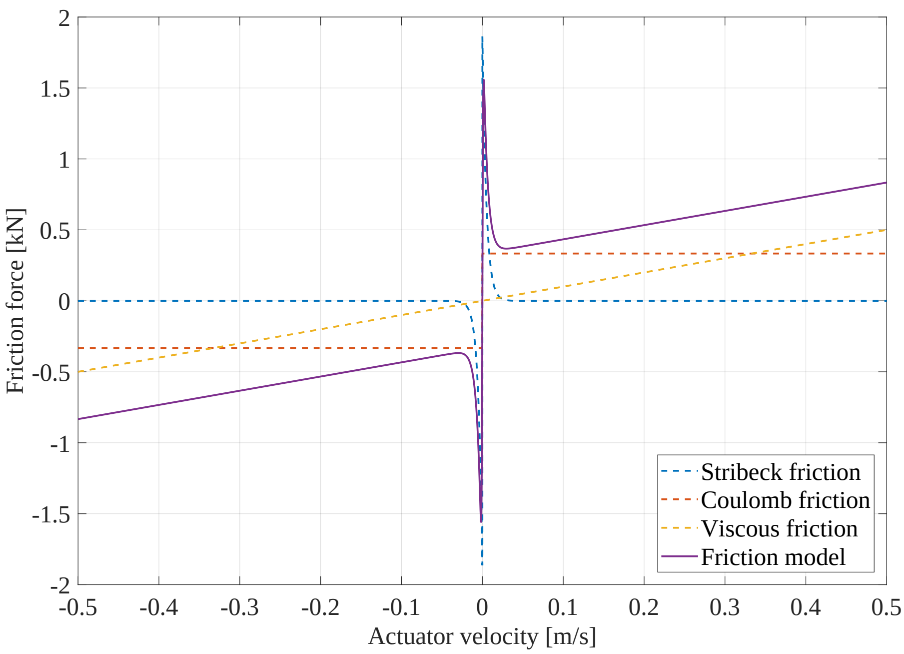

Figure 4.7. Modelled friction force as function of piston velocity.

Load Modelling

As described in Chapter 2, the desired load characteristics are a load of high inertia and high stiffness. Such a load may be described as a mass, spring, damper system. As the sliding mass has been considered as a part of the system the external force acting on it will be described by a spring force and a damping.

$$F_{\mathrm{ext}} = -b_{\mathrm{p}}\dot{x}_{\mathrm{p}} - k_{\mathrm{s}}x_{\mathrm{p}} \tag{4.15}$$

The exact magnitude of the external force is not important since the force only serves to represent some generic test object with the described characteristics. However the magnitude of the force should be in a region that offers resistance to the applied hydraulic force but still allows the cylinder to travel along most of its stroke length. To approximate the spring constant the maximum load force is calculated by Equation 4.16.

$$F_{\mathrm{max}} = p_{\mathrm{S}}A_{\mathrm{A}} - p_{\mathrm{T}}A_{\mathrm{B}} = 125\mathrm{kN} \tag{4.16}$$

The corresponding spring constant is found by Equation 4.17.

$$k_{\mathrm{s,max}} = \frac{F_{\mathrm{max}}}{x_{\mathrm{p,max}}} = 358\frac{\mathrm{kN}}{\mathrm{m}} \tag{4.17}$$

To avoid reaching the end stops a spring constant in the region of 400kN/m will be used.

Non Linear System Model

The model of the servo actuator system is thereby constituted of three differential equations and two algebraic equations as seen in equations 4.18 - 4.22. Additionally the valve spool dynamic are included in the model.

$$\ddot{x}_{\mathrm{p}} = \frac{1}{M_{\mathrm{tot}}}\left(p_{\mathrm{B}}A_{\mathrm{B}} - p_{\mathrm{A}}A_{\mathrm{A}} - F_{\mathrm{fr}} + F_{\mathrm{ext}}\right) \tag{4.18}$$

$$\dot{p}_{\mathrm{A}} = \frac{\beta(p_{\mathrm{A}})}{V_{\mathrm{A0}} - x_{\mathrm{p}}A_{\mathrm{A}}}\left(Q_{\mathrm{A}} - C_{\mathrm{le}}(p_{\mathrm{A}} - p_{\mathrm{B}}) + \dot{x}_{\mathrm{p}}A_{\mathrm{A}}\right) \tag{4.19}$$

$$\dot{p}_{\mathrm{B}} = \frac{\beta(p_{\mathrm{B}})}{V_{\mathrm{B0}} + x_{\mathrm{p}}A_{\mathrm{B}}}\left(C_{\mathrm{le}}(p_{\mathrm{A}} - p_{\mathrm{B}}) - Q_{\mathrm{B}} - \dot{x}_{\mathrm{p}}A_{\mathrm{B}}\right) \tag{4.20}$$

$$\begin{aligned} Q_{\mathrm{A}} = {} & k_{\mathrm{vA}}x_{\mathrm{v}}\sqrt{|p_{\mathrm{S}} - p_{\mathrm{A}}|}\mathrm{sgn}(p_{\mathrm{S}} - p_{\mathrm{A}})(x_{\mathrm{v}} \geq 0) \\ & + k_{\mathrm{vA}}x_{\mathrm{v}}\sqrt{|p_{\mathrm{A}} - p_{\mathrm{T}}|}\mathrm{sgn}(p_{\mathrm{A}} - p_{\mathrm{T}})(x_{\mathrm{v}} < 0) \end{aligned} \tag{4.21}$$

$$\begin{aligned} Q_{\mathrm{B}} = {} & k_{\mathrm{vB}}x_{\mathrm{v}}\sqrt{|p_{\mathrm{B}} - p_{\mathrm{T}}|}\mathrm{sgn}(p_{\mathrm{B}} - p_{\mathrm{T}})(x_{\mathrm{v}} \geq 0) \\ & + k_{\mathrm{vB}}x_{\mathrm{v}}\sqrt{|p_{\mathrm{S}} - p_{\mathrm{B}}|}\mathrm{sgn}(p_{\mathrm{S}} - p_{\mathrm{B}})(x_{\mathrm{v}} < 0) \end{aligned} \tag{4.22}$$

4.1.3 Model Structure

To simulate the system behaviour the model is implemented in Simulink. The overall model structure is seen in Figure 4.8.

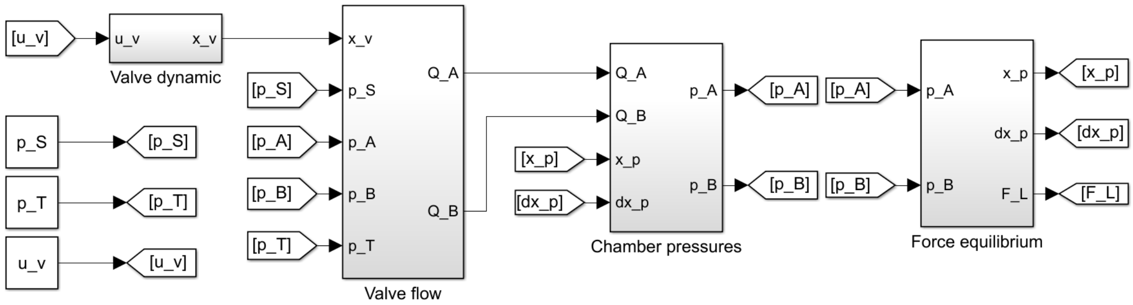

Figure 4.8. Model structure in Simulink.

Assumptions made when implementing the model:

- Constant supply and tank pressures.
- Constant bulk modulus.
- No internal leakage flow in the actuator.

The validity of these assumptions are later investigated. To investigate if the modelled system depicts the behaviour of the actual system a validation of the model is conducted in the following section.

4.1.4 Model Validation

This section contains a validation of the derived model to investigate if it sufficiently depicts the behaviour of the actual system. The necessary model accuracy depends on what the model is to be used for. For the purpose of designing a force controller the model dynamics should depict the actual system decently, however small deviations may be corrected for by the controller. It is not possible to measure the force exerted directly on the piston due to the force transducer being installed between the main cylinder and the sliding mass as depicted in Figure 2.2. For this reason the sliding mass is included in the model. The part of the system seen in Figure 2.2 that is to be validated is thereby seen in Figure 4.9.

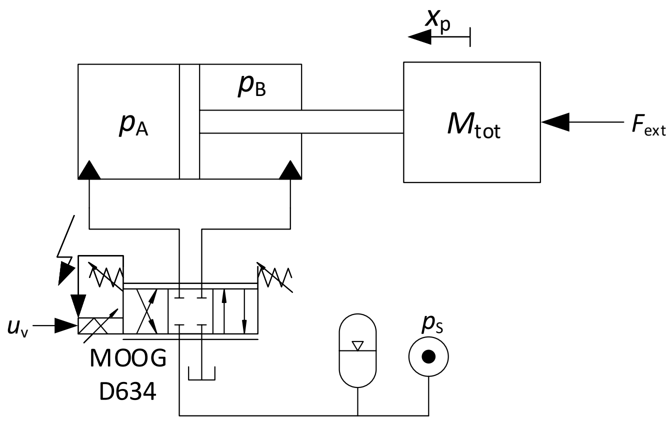

Figure 4.9. Diagram of the system to be validated.

Due to the mass of the pistons and the sliding mass all being connected on the same axis and assumed rigid the acceleration of the total moving mass M_{tot} are assumed uniform. It is assumed that no leakage flow occurs in the actuator. This is considered a valid assumption since the actuators are rather new and sealings usually are highly efficient.

The validation is carried out in the following way. As seen in the figure the system takes three inputs being the valve signal, supply pressure and applied force from the main cylinder. The valve signal is stepped by 2 % in both positive and negative spool direction while the supply pressure is set constant and the force from the main cylinder acting on the sliding mass is adjusted so that the mass will not reach either endstop while performing the sequence. The valve signal, supply pressure and force are logged along with the piston position, piston velocity, piston side chamber pressure and rod side chamber pressure.

Parameters such as cylinder dimensions, masses and areas are considered hard parameters and thereby assumed to be fixed values and can be seen in Appendix A. Soft parameters are values that may vary with system condition and may thereby be difficult to determine. By comparing the behaviour of the model to the actual system behaviour soft parameters may be approximated by carefully adapting these so that the behaviour of the modelled system corresponds with that of the actual system. The soft parameters in the model are the bulk modulus and the friction force parameters. When comparing the simulated system behaviour with the actual system behaviour the soft parameters have been given the values listed in table 4.2.

Parameter	Value
β	$8000 \cdot 10^5$ Pa
b_{v}	100 kNs/m
F_{c}	300 N
F_{s}	700 N
γ	0.001
c_{s}	$5 \cdot 10^{-3}$

Table 4.2. Soft parameters approximated by comparing system behaviour.

The logged valve signal, supply pressure and force are seen in Figure 4.10 and are used as input in the model to compare the behaviour of the modelled system with that of the actual system. The comparison of the actual system behaviour with the simulated system behaviour is seen in Figure 4.11.

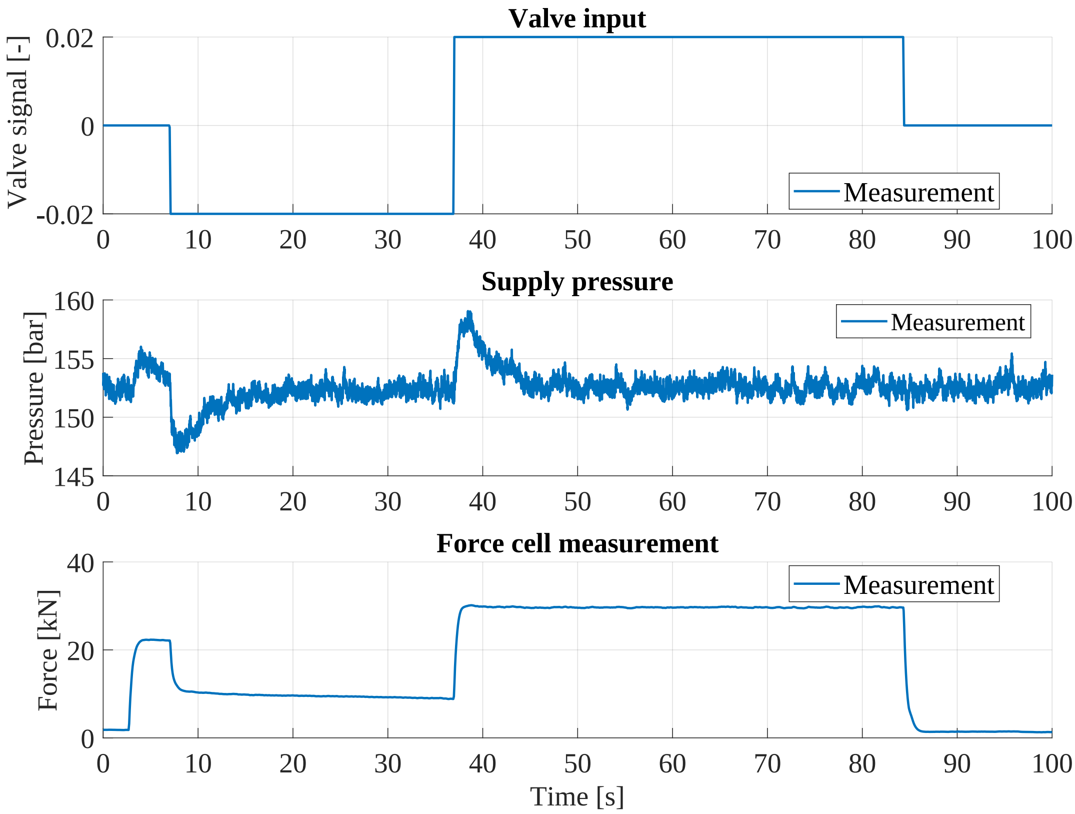

Figure 4.10. Input to the system and model.

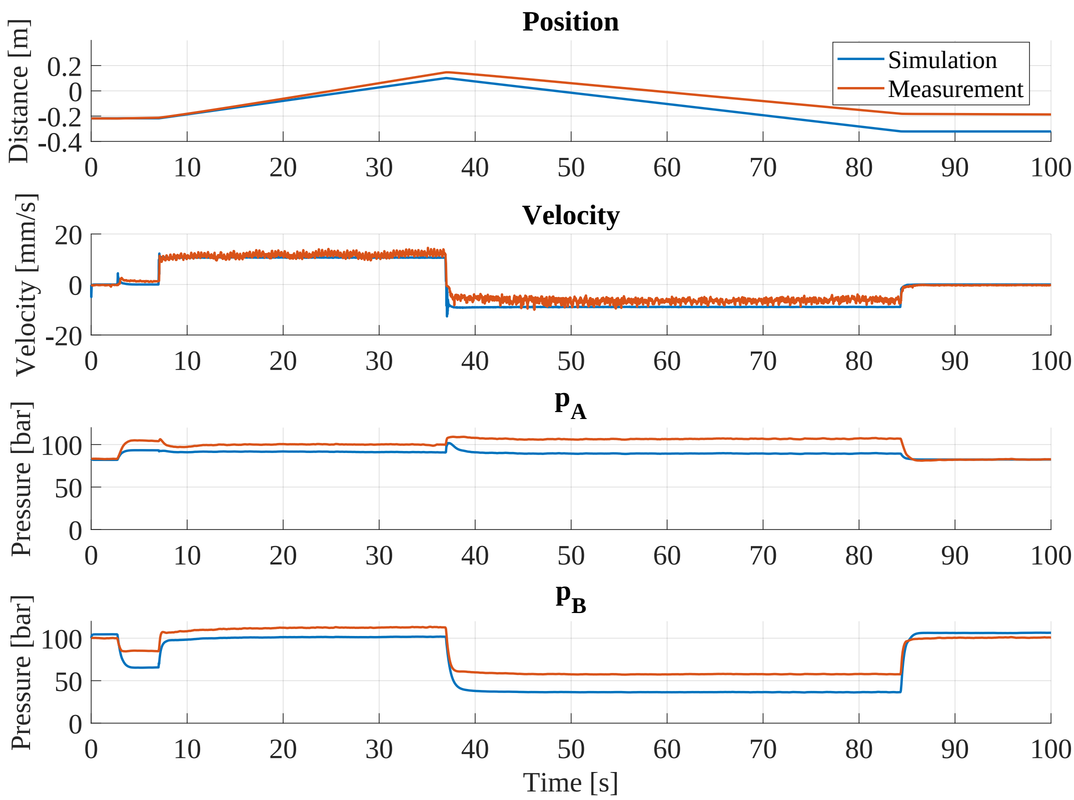

Figure 4.11. Measured output from the system plotted with simulated output.

The simulated piston position and velocity show coherence with the measured however with some deviation. The simulated velocity seem to be too slow when given a negative valve signal while it seem to be too fast when given a positive valve signal which is confirmed by the piston position as it is seen to travel shorter and longer than the measured, for negative and positive valve signal respectively. This indicate that there is some deviation in the simulated forces. As the friction force in the system is difficult to determine it is possible that this is the source of error. It is however hard to tune the friction force to fit the measurements better since it should then be reduced for negative valve signal while it should be increased for positive valve signal.

The deviation in piston position and velocity could also be a result of the valve spool having a small offset. As the valve spool moves back and forth in the valve it may not always be in the exact neutral position even though a valve signal corresponding to the neutral position is given. By comparing the piston position in Figure 4.11 with the valve signal in Figure 4.10 it seems plausible that the valve spool during the measurements had a small offset in the negative direction. This is suggested since the measurements show a faster velocity for negative valve signal than that of the simulated while showing a slower velocity at positive valve signal.

The simulated chamber pressures are seen to show the same tendencies as the measured chamber pressures however with some deviation as well. The transient areas are seen to correspond decently however with some differences in the magnitude of the pressures. In steady state the simulated pressures are seen to have an offset. This offset is of varying magnitude but common is that the simulated pressures reach lower steady state values than the measured pressures.

It should be mentioned that the magnitude of the bulk modulus and friction force given in table 4.2 are uncertain to some extent. That is because these values may be varied but the system behaviour seen in Figure 4.11 is still obtained. Especially the viscous damping coefficient is uncertain as the system behaviour does not change significantly while varying the coefficient between 50 kNs/m and 200 kNs/m. To account for this the influence of these soft parameters are investigated in Chapter 5.

Based on this validation it is concluded that the proposed model depicts the system sufficiently as the controller will eliminate some of the deviation seen such as the steady state error in the pressures.

4.2 Reduced Order Model

To simplify the analysis of the system a reduced order model is derived, following the procedure as described by Hansen et al. [2016]. The simplifications and assumptions applied in the derivation of the reduced order model and the following linear model are here summarised:

1. No leakage flow.
2. Steady state flow conditions.
3. Stribeck and coulomb friction components neglected.
4. Chamber volumes assumed constant around the linearisation point.

Let the cylinder area ratio be defined as Equation 4.23 and the valve flowpath ratio as Equation 4.24.

$$\alpha = \frac{A_\mathrm{B}}{A_\mathrm{A}} \tag{4.23}$$

$$\sigma = \frac{k_\mathrm{vB}}{k_\mathrm{vA}} \tag{4.24}$$

Using the cylinder area ratio definition it is possible to define the load force as the hydraulic force delivered by the piston as seen in Equation 4.25. Furthermore the load pressure is defined as the virtual pressure proportional to the load force as seen in Equation 4.26.

$$F_\mathrm{L} = p_\mathrm{A} A_\mathrm{A} - p_\mathrm{B} A_\mathrm{B} = A_\mathrm{A}(p_\mathrm{A} - \alpha p_\mathrm{B}) = A_\mathrm{A} p_\mathrm{L} \tag{4.25}$$

$$p_\mathrm{L} = p_\mathrm{A} - \alpha p_\mathrm{B} \tag{4.26}$$

Using the definition of load pressure the piston acceleration can be formulated as seen in Equation 4.27.

$$\ddot{x}_\mathrm{p} = \frac{1}{M}\big(-p_\mathrm{L} A_\mathrm{A} - F_\mathrm{fr} + F_\mathrm{ext}\big) \tag{4.27}$$

The load pressure gradient is defined as seen in Equation 4.28. By substituting the continuity equations formulated for the pressure gradients $\dot{p}_\mathrm{A}$ (4.19) and $\dot{p}_\mathrm{B}$ (4.20) the load pressure gradient may be expressed more explicit as seen in Equation 4.29.

$$\dot{p}_\mathrm{L} = \dot{p}_\mathrm{A} - \alpha \dot{p}_\mathrm{B} \tag{4.28}$$

$$\dot{p}_\mathrm{L} = \frac{\beta}{V_\mathrm{A}(x_\mathrm{p})}\big(Q_\mathrm{A} + A_\mathrm{A}\dot{x}_\mathrm{p}\big) - \alpha\frac{\beta}{V_\mathrm{B}(x_\mathrm{p})}\big(-Q_\mathrm{B} - A_\mathrm{B}\dot{x}_\mathrm{p})\big) \tag{4.29}$$

The ratio of the flow to the cylinder chambers is equal to the ratio of the piston areas when assuming steady state flow conditions. The flow to the rod side Q_B may then be expressed as

$$Q_\mathrm{B} = \alpha Q_\mathrm{A} \tag{4.30}$$

Utilising this relation the load pressure gradient may finally be formulated as

$$\dot{p}_{\mathrm{L}} = \underbrace{\left(\frac{\beta}{V_{\mathrm{A}}(x_{\mathrm{p}})} + \alpha^2 \frac{\beta}{V_{\mathrm{B}}(x_{\mathrm{p}})}\right)}_{C_{\mathrm{H}}} (Q_{\mathrm{A}} + A_{\mathrm{A}} \dot{x}_{\mathrm{p}}) \tag{4.31}$$

Now the expression for the valve flow is manipulated so that it depends on the load pressure rather than the chamber pressures. Again utilising the steady state flow conditions assumption the following relationship between the system pressures is derived:

$$Q_{\mathrm{B}} = \alpha Q_{\mathrm{A}} \tag{4.32}$$

$$k_{\mathrm{vB}} x_{\mathrm{v}} \sqrt{p_{\mathrm{B}} - p_{\mathrm{T}}} = \alpha k_{\mathrm{vA}} x_{\mathrm{v}} \sqrt{p_{\mathrm{S}} - p_{\mathrm{A}}} \tag{4.33}$$

$$\frac{\sigma^2}{\alpha^2}(p_{\mathrm{B}} - p_{\mathrm{T}}) = p_{\mathrm{S}} - p_{\mathrm{A}} \tag{4.34}$$

From this the chamber pressures p_{A} and p_{B} can be expressed as functions of supply, tank and load pressures as seen in equations 4.35 and 4.36.

$$p_{\mathrm{A}} = \frac{\alpha^3 p_{\mathrm{S}} + \sigma^2 p_{\mathrm{L}} + \sigma^2 \alpha p_{\mathrm{T}}}{\sigma^2 + \alpha^3}\ , \text{ for } x_{\mathrm{v}} \geq 0 \tag{4.35}$$

$$p_{\mathrm{B}} = \frac{\alpha^2 p_{\mathrm{S}} - \alpha^2 p_{\mathrm{L}} + \sigma^2 p_{\mathrm{T}}}{\sigma^2 + \alpha^3}\ , \text{ for } x_{\mathrm{v}} \geq 0 \tag{4.36}$$

Repeating this process for negative valve spool position yields the following expressions for the chamber pressures:

$$p_{\mathrm{A}} = \frac{\sigma^2 p_{\mathrm{L}} + \alpha \sigma^2 p_{\mathrm{S}} + \alpha^3 p_{\mathrm{T}}}{\sigma^2 + \alpha^3}\ , \text{ for } x_{\mathrm{v}} < 0 \tag{4.37}$$

$$p_{\mathrm{B}} = \frac{\sigma^2 p_{\mathrm{S}} - \alpha^2 p_{\mathrm{L}} + \alpha^2 p_{\mathrm{T}}}{\sigma^2 + \alpha^3}\ , \text{ for } x_{\mathrm{v}} < 0 \tag{4.38}$$

By substituting the expression for the chamber pressure into the expression for the valve flow for positive valve spool position yields

$$Q_{\mathrm{A}} = k_{\mathrm{vA}} x_{\mathrm{v}} \sqrt{p_{\mathrm{S}} - p_{\mathrm{A}}}\ , \text{ for } x_{\mathrm{v}} \geq 0 \tag{4.39}$$

$$Q_{\mathrm{A}} = k_{\mathrm{vA}} x_{\mathrm{v}} \sqrt{p_{\mathrm{S}} - \frac{\alpha^3 p_{\mathrm{S}} + \sigma^2 p_{\mathrm{L}} + \sigma^2 \alpha p_{\mathrm{T}}}{\sigma^2 + \alpha^3}}\ , \text{ for } x_{\mathrm{v}} \geq 0 \tag{4.40}$$

$$Q_{\mathrm{A}} = k_{\mathrm{vA}} x_{\mathrm{v}} \sqrt{\frac{\sigma^2 + \alpha^3}{\sigma^2 + \alpha^3} p_{\mathrm{S}} - \frac{\alpha^3 p_{\mathrm{S}} + \sigma^2 p_{\mathrm{L}} + \sigma^2 \alpha p_{\mathrm{T}}}{\sigma^2 + \alpha^3}} \text{ , for } x_{\mathrm{v}} \geq 0 \tag{4.41}$$

$$Q_{\mathrm{A}} = k_{\mathrm{vA}} x_{\mathrm{v}} \sqrt{\frac{\sigma^2 p_{\mathrm{S}} - \sigma^2 p_{\mathrm{L}} - \sigma^2 \alpha p_{\mathrm{T}}}{\sigma^2 + \alpha^3}} \text{ , for } x_{\mathrm{v}} \geq 0 \tag{4.42}$$

$$Q_{\mathrm{A}} = k_{\mathrm{vA}} x_{\mathrm{v}} \sigma \sqrt{\frac{p_{\mathrm{S}} - p_{\mathrm{L}} - \alpha p_{\mathrm{T}}}{\sigma^2 + \alpha^3}} \text{ , for } x_{\mathrm{v}} \geq 0 \tag{4.43}$$

Following the same procedure for negative valve spool position yields

$$Q_{\mathrm{A}} = k_{\mathrm{vA}} x_{\mathrm{v}} \sigma \sqrt{\frac{\alpha p_{\mathrm{S}} + p_{\mathrm{L}} - p_{\mathrm{T}}}{\sigma^2 + \alpha^3}} \text{ , for } x_{\mathrm{v}} < 0 \tag{4.44}$$

The reduced order model is thereby constituted by the following three expressions:

$$\ddot{x}_{\mathrm{p}} = \frac{1}{M}\big(- p_{\mathrm{L}} A_{\mathrm{A}} - F_{\mathrm{fr}} + F_{\mathrm{ext}}\big) \tag{4.45}$$

$$\dot{p}_{\mathrm{L}} = C_{\mathrm{H}}(Q_{\mathrm{A}} + A_{\mathrm{A}} \dot{x}_{\mathrm{p}}) \tag{4.46}$$

$$Q_{\mathrm{A}} = \frac{k_{\mathrm{vA}} x_{\mathrm{v}} \sigma}{\sqrt{\sigma^2 + \alpha^3}} \begin{cases} \sqrt{p_{\mathrm{S}} - p_{\mathrm{L}} - \alpha p_{\mathrm{T}}} \text{ , for } x_{\mathrm{v}} \geq 0 \\ \sqrt{\alpha p_{\mathrm{S}} + p_{\mathrm{L}} - p_{\mathrm{T}}} \text{ , for } x_{\mathrm{v}} < 0 \end{cases} \tag{4.47}$$

The derivation of the reduced order model lead to a decrease in the system order of one.

4.3 Linear Model

To analyse the frequency response of the system the reduced order model is linearised. The valve flow described by the orifice equation is non linear due to the square root function and is approximated by a first order Taylor series expansion as seen in Equation 4.48.

$$\widetilde{Q}_{\mathrm{A}} = Q_{\mathrm{A0}} + \left.\frac{\partial Q_{\mathrm{A}}}{\partial x_{\mathrm{v}}}\right|_0 (x_{\mathrm{v}} - x_{\mathrm{v0}}) + \left.\frac{\partial Q_{\mathrm{A}}}{\partial p_{\mathrm{L}}}\right|_0 (p_{\mathrm{L}} - p_{\mathrm{L0}}) \tag{4.48}$$

$\widetilde{Q}_{\mathrm{A}}$ is now approximated as a Taylor series. However it is still not linear and is therefore expressed in change variables:

$$\widetilde{Q}_{\mathrm{A}} - Q_{\mathrm{A0}} = \Delta Q_{\mathrm{A}} = \left.\frac{\partial Q_{\mathrm{A}}}{\partial x_{\mathrm{v}}}\right|_0 \Delta x_{\mathrm{v}} + \left.\frac{\partial Q_{\mathrm{A}}}{\partial p_{\mathrm{A}}}\right|_0 \Delta p_{\mathrm{A}} \tag{4.49}$$

$$\Delta Q_\mathrm{A} = k_\mathrm{qx}\Delta x_\mathrm{v} + k_\mathrm{qp}\Delta p_\mathrm{L} \tag{4.50}$$

With the linearisation konstants

$$k_\mathrm{qx} = \frac{k_\mathrm{vA}\sigma}{\sqrt{\sigma^2+\alpha^3}}\begin{cases}\sqrt{p_\mathrm{S}-p_\mathrm{L0}-\alpha p_\mathrm{T}} & \text{, for } x_\mathrm{v} \geq 0\\ \sqrt{\alpha p_\mathrm{S}+p_\mathrm{L0}-p_\mathrm{T}} & \text{, for } x_\mathrm{v} < 0\end{cases} \tag{4.51}$$

$$k_\mathrm{qp} = \frac{k_\mathrm{vA}x_\mathrm{v0}\sigma}{\sqrt{\sigma^2+\alpha^3}}\begin{cases}\frac{-1}{2\sqrt{p_\mathrm{S}-p_\mathrm{L0}-\alpha p_\mathrm{T}}} & \text{, for } x_\mathrm{v} \geq 0\\ \frac{1}{2\sqrt{\alpha p_\mathrm{S}-p_\mathrm{L0}-p_\mathrm{T0}}} & \text{, for } x_\mathrm{v} < 0\end{cases} \tag{4.52}$$

The flow Q_A is now linearised. The expression for the load pressure gradient is non linear due to the change in chamber volumes with piston position. This non linearity is eliminated by assuming the volume changes at or close to the linearisation point to be small thereby considering the chamber volumes as constant. The expression for the piston movement is non linear due to the Stribeck and Coulomb friction force components. The expression is linearised by considering these components as a disturbance and neglecting them in the system. The linear model is thereby constituted by equations 4.54, 4.53 and 4.55.

$$\Delta\ddot{x}_\mathrm{p} = \frac{1}{M}\big(-\Delta p_\mathrm{L}A_\mathrm{A} - b_\mathrm{v}\Delta\dot{x}_\mathrm{p} + F_\mathrm{ext}\big) \tag{4.53}$$

$$\Delta\dot{p}_\mathrm{L} = C_\mathrm{H}(\Delta Q_\mathrm{A} + A_\mathrm{A}\dot{x}_\mathrm{p}) \tag{4.54}$$

$$\Delta Q_\mathrm{A} = k_\mathrm{qx}\Delta x_\mathrm{v} + k_\mathrm{qp}\Delta p_\mathrm{L} \tag{4.55}$$

The linear model describes the change in variables from the linearisation point. Hence, the non linear model values may be approximated by adding the change in variables to the linearisation point values as seen in Equation 4.56.

$$\widetilde{\boldsymbol{x}} = \Delta\boldsymbol{x} + \boldsymbol{x}_0 \tag{4.56}$$

Where $\Delta\boldsymbol{x}$ are the change in values in the linear model and $\boldsymbol{x}_0$ are the variable values at the linearisation point. By this the nonlinear model values are approximated as

$$\widetilde{x}_\mathrm{p} = \Delta x_\mathrm{p} + x_\mathrm{p} \tag{4.57}$$

$$\widetilde{\dot{x}}_\mathrm{p} = \Delta\dot{x}_\mathrm{p} + \dot{x}_\mathrm{p0} \tag{4.58}$$

$$\widetilde{p}_\mathrm{L} = \Delta p_\mathrm{L} + p_\mathrm{L0} \tag{4.59}$$

However the linear model approximation is only valid at or close to the linearisation point. Depending on the non linearity of the system, the error between the approximated values and the actual values will increase as the interval Δ is increased.

Control Design 5

This chapter contains design and implementation of a force controller in the hydraulic servo actuator system and an analysis of the controller performance.

5.1 Force Controller

General for hydraulic systems are that their behaviour often is non linear. Nevertheless linear control theory is often applied in the control design of such systems, due to this being the conventional strategy but also because it requires minimal system feedback. The most simple control strategy is to design a simple controller, often a P or a PI controller, and let it act on the error of the desired control variable and thereby control the input to the system. In this case the controller would act on the error of the force and control the valve spool position in the system accordingly as seen in Figure 5.1.

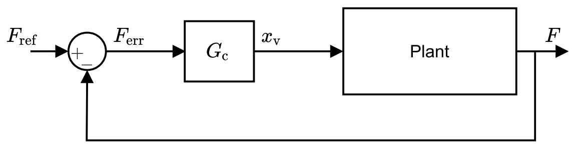

Figure 5.1. Closed loop force control with linear controller.

Which force in the system that is to be controlled depends on the application and the accessible measurements for the closed loop control. In the back-to-back cylinder test bench in the laboratory the resulting force on the sliding mass is measured as described in Chapter 2 and may be used as feedback in a control loop. However this is not a possibility in most test benches designed by R&D A/S due to the applied forces being out of range for most force transducers. Instead the hydraulic force delivered is estimated from pressure measurements which is also the case for the HALT test bench described in Chapter 1. This force is denoted the load force and defined as the force proportional to the load pressure as seen in Equation 5.1.

$$F_{\text{L}} = p_{\text{L}} A_{\text{A}} \tag{5.1}$$

5.1.1 System Transfer Function

By assuming the initial conditions to be zero, that is $\dot{x}_{\text{p}}(0) = x_{\text{p}}(0) = p_{\text{L}}(0) = 0$, the linear model may be formulated in the Laplace domain as seen in equations 5.2 - 5.4.

$$X_\mathrm{p}(s) = \frac{1}{Ms^2 + b_\mathrm{v}s}(-P_\mathrm{L}(s)A_\mathrm{A} + F_\mathrm{ext}(s)) \tag{5.2}$$

$$P_\mathrm{L}(s) = \frac{C_\mathrm{H}}{s}(Q_\mathrm{A}(s) + A_\mathrm{A}sX_\mathrm{p}(s)) \tag{5.3}$$

$$Q_\mathrm{A}(s) = k_\mathrm{qx}X_\mathrm{v}(s) + k_\mathrm{qp}P_\mathrm{L}(s) \tag{5.4}$$

The Laplace transformed model is seen as a block diagram in Figure 5.2. The valve dynamic has not been included as it is assumed to be faster than the system dynamic. Whether this is a fair assumption will be investigated in this section.

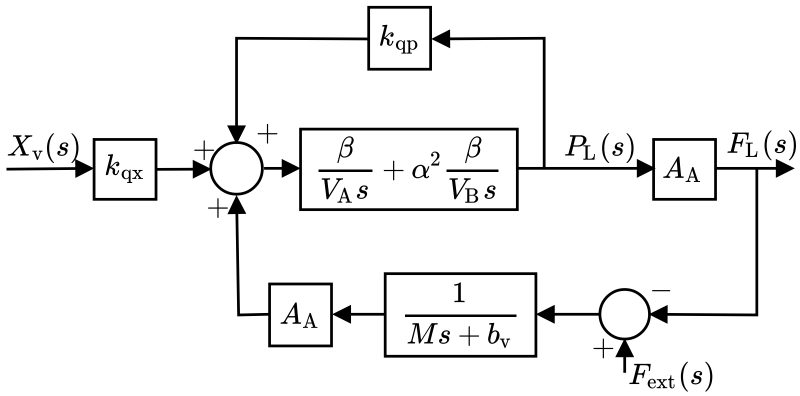

Figure 5.2. Block diagram of the linear model.

By substituting the expression for the piston position (5.2) and the expression for the flow (5.4) into the expression for the load pressure (5.3) yields the following expression for the load pressure:

$$P_\mathrm{L}(s) = \frac{C_\mathrm{H}(Mk_\mathrm{qx}s + b_\mathrm{v}k_\mathrm{qx})X_\mathrm{v}(s) + C_\mathrm{H}A_\mathrm{A}F_\mathrm{ext}(s)}{Ms^2 + (b_\mathrm{v} - C_\mathrm{H}Mk_\mathrm{qp})s + A_\mathrm{A}^2C_\mathrm{H} - C_\mathrm{H}b_\mathrm{v}k_\mathrm{qp}} \tag{5.5}$$

By substituting this expression for the load pressure into Equation 5.1 the transfer function for the load force system is obtained as seen in Equation 5.6.

$$F_\mathrm{L}(s) = \frac{A_\mathrm{A}C_\mathrm{H}(Mk_\mathrm{qx}s + b_\mathrm{v}k_\mathrm{qx})X_\mathrm{v}(s) + C_\mathrm{H}A_\mathrm{A}^2F_\mathrm{ext}(s)}{Ms^2 + (b_\mathrm{v} - C_\mathrm{H}Mk_\mathrm{qp})s + A_\mathrm{A}^2C_\mathrm{H} - C_\mathrm{H}b_\mathrm{v}k_\mathrm{qp}} \tag{5.6}$$

From the transfer function (5.6) it can be seen that the load force depends on two inputs, which are the valve spool position $X_\mathrm{v}(s)$ and the external force acting on the piston $F_\mathrm{ext}(s)$. However only one input is permitted in transfer function analysis. By considering the external force as a disturbance to the system it is neglected and the transfer function from valve spool position to load force may be formulated as:

$$G_{\mathrm{Fx}}(s) = \frac{F_{\mathrm{L}}(s)}{X_{\mathrm{v}}(s)} = \frac{A_{\mathrm{A}} C_{\mathrm{H}} (M k_{\mathrm{qx}} s + b_{\mathrm{v}} k_{\mathrm{qx}})}{M s^2 + (b_{\mathrm{v}} - C_{\mathrm{H}} M k_{\mathrm{qp}}) s + A_{\mathrm{A}}^2 C_{\mathrm{H}} - C_{\mathrm{H}} b_{\mathrm{v}} k_{\mathrm{qp}}} \tag{5.7}$$

The transfer function denominator has the characteristics of a second order system. However a zero can be seen in the numerator.

By multiplying the transfer function describing the valve dynamic (4.11) with the transfer function derived for the valve spool position to load force system (5.7) the transfer function for the valve signal to load force system, and thereby the transfer function for the entire system, may be expressed by Equation 5.8.

$$G_{\mathrm{Fu}}(s) = \frac{F_{\mathrm{L}}(s)}{U_{\mathrm{v}}(s)} = \frac{X_{\mathrm{v}}(s)}{U_{\mathrm{v}}(s)} \cdot \frac{F_{\mathrm{L}}(s)}{X_{\mathrm{v}}(s)} = \frac{A_{\mathrm{A}} C_{\mathrm{H}} M k_{\mathrm{qx}} \omega_{\mathrm{n}}^2 s + A_{\mathrm{A}} C_{\mathrm{H}} b_{\mathrm{v}} k_{\mathrm{qx}} \omega_{\mathrm{n}}^2}{M s^4 + k_1 s^3 + k_2 s^2 + k_3 s + k_4} \tag{5.8}$$

with

$$\begin{aligned}
k_1 &= (2\zeta M \omega_{\mathrm{n}} - C_{\mathrm{H}} M k_{\mathrm{qp}} + b_{\mathrm{v}}) \\
k_2 &= (2\zeta b_{\mathrm{v}} \omega_{\mathrm{n}} + A_{\mathrm{A}}^2 C_{\mathrm{H}} + M \omega_{\mathrm{n}}^2 - 2\zeta C_{\mathrm{H}} M k_{\mathrm{qp}} \omega_{\mathrm{n}} - C_{\mathrm{H}} b_{\mathrm{v}} k_{\mathrm{qp}}) \\
k_3 &= (2 A_{\mathrm{A}}^2 \zeta C_{\mathrm{H}} \omega_{\mathrm{n}} - 2\zeta C_{\mathrm{H}} b_{\mathrm{v}} k_{\mathrm{qp}} \omega_{\mathrm{n}} - C_{\mathrm{H}} M k_{\mathrm{qp}} \omega_{\mathrm{n}}^2 + b_{\mathrm{v}} \omega_{\mathrm{n}}^2) \\
k_4 &= A_{\mathrm{A}}^2 C_{\mathrm{H}} \omega_{\mathrm{n}}^2 - C_{\mathrm{H}} b_{\mathrm{v}} k_{\mathrm{qp}} \omega_{\mathrm{n}}^2
\end{aligned} \tag{5.9}$$

By comparing the two transfer functions it is evidently seen that including the valve dynamic in the system transfer function results in a more complicated transfer function. By assuming that the valve dynamic is faster than the rest of the system it may be neglected and a controller may be designed from the simpler valve spool position to load force system. It is however not known if this is a fair assumption and it is therefore investigated in the following section.

5.1.2 Frequency Response Analysis

To investigate the system behaviour a frequency analysis is conducted. As described in Chapter 4 the linear model is only valid at or close to the linearisation point. The linearisation point values are found by choosing a representative velocity and then calculate the corresponding steady state values. The steady state values are calculated from the non linear model equations by setting the gradients equal to zero. The piston position is independent and chosen at $x_{\mathrm{p}} = 0$ m since the the piston is assumed to be working around the middle point rather than at the end stops. As the cylinder is assumed to move back and forth during a work cycle the piston velocity is not likely to be zero but it is also assumed that it does move slowly why the piston velocity is expected to be low. The initial valve spool position and load pressure are thereby calculated corresponding to a piston velocity of $\dot{x}_{\mathrm{p}} = 0.1$ m/s. The piston position and velocity are considered representative for how the system is expected to be operated. The linear model is thereby evaluated at the linearisation point given as:

$$\boldsymbol{x}_0 = [\ x_{\mathrm{p0}} = 0 \text{ m}\ ,\ x_{\mathrm{v0}} = 0.17\ ,\ p_{\mathrm{L0}} = -20.6 \text{ bar}\ ] \tag{5.10}$$

The bode plot for the valve spool position to load force system, as seen in Equation 5.7, for varying piston position linearisation points is seen in Figure 5.3 using the system values listed in table 5.1.

Variable	Value	Unit
D/d/L	80/40/700	mm
V_{A0}	1.910	l
V_{B0}	1.471	l
M_{tot}	730	kg
β	8000	bar
b_v	100	kNs/m

Table 5.1. System values used for plotting the bode plot.

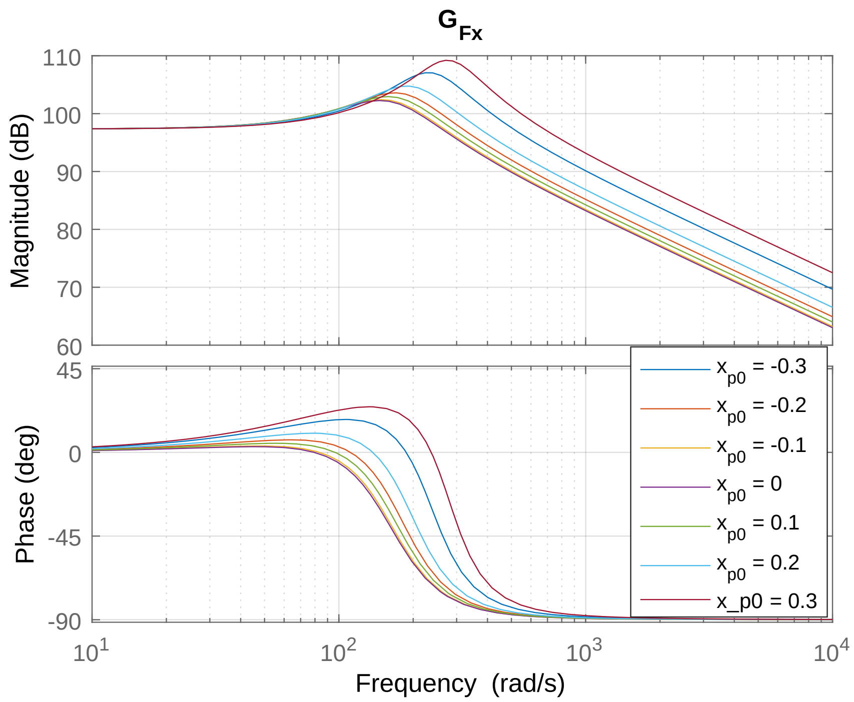

Figure 5.3. Bode plot for the valve spool position to load force system.

From the bode plot it can be seen that the system magnitude shows the behaviour of a second order system with a resonance peak around the break away frequency which increases with linearisation points moving towards the end stops. It can also be seen that the system bandwidth increases when the linearisation point moves towards the end stops. The phase however is seen to shift 90° indicating first order system behaviour. The contribution from the zero is seen to influence the system most at linearisation points close to the end stops.

When the model is linearised with the piston in the middle position the system is seen to be the slowest with a bandwidth of approximately 25 Hz. From the bode plot slightly different behaviour is observed for linearisation points of equal magnitude but with different sign. This is concluded to be a result of the cylinder being asymmetrically constructed as this results in different chamber volumes at piston positions of equal magnitude but with different sign which at last results in different pressure dynamics. It thereby indicates that the lowest bandwidth of the system is not when the piston is in the exact middle position but rather when it is shifted slightly to the side. The influence of this property is however assumed to be negligible and the linearisation point for the piston position will still be chosen in the middle position ($x_{p0} = 0$ m). To investigate if the valve dynamic influences the system behaviour the bode plot for the valve signal to load force system, as seen in Equation 5.8, is plotted in Figure 5.4 along with the bode plot for the valve spool position to load force system both linearised with the piston in the middle position ($x_{p0} = 0$ m).

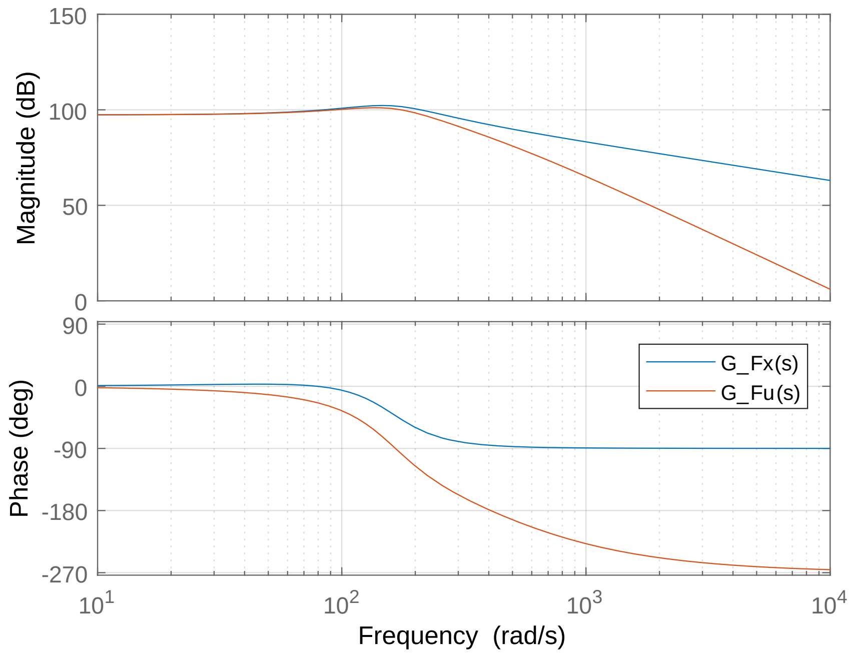

Figure 5.4. Bode plot for the valve spool position to load force system and the valve signal to load force system, respectively..

From the bode plot for the valve signal to load force system it can be seen that the gain at low frequencies is approximately equal to that of the valve spool position to load force system. Around the system break away frequency it can be seen that the system is slightly more damped than the spool position to force system. Furthermore a phase shift of -270 ° is introduced resulting in a negative gain margin for the system and thus indicating system instability for the closed loop system. To investigate this issue the root locus for the valve signal to load force system is plotted in Figure 5.5.

From the root locus it is confirmed that the complex conjugated poles will be placed in the right half plane for a gain greater than 5.5e-5 $\frac{1}{\mathrm{N}}$ and thus making the system unstable. This gain seem to have a small magnitude. It does however seem realistic by recalling that the gain scales the normalised valve signal ranging between -1 and 1 corresponding to the error on the force which for the system may be in the range of kN.

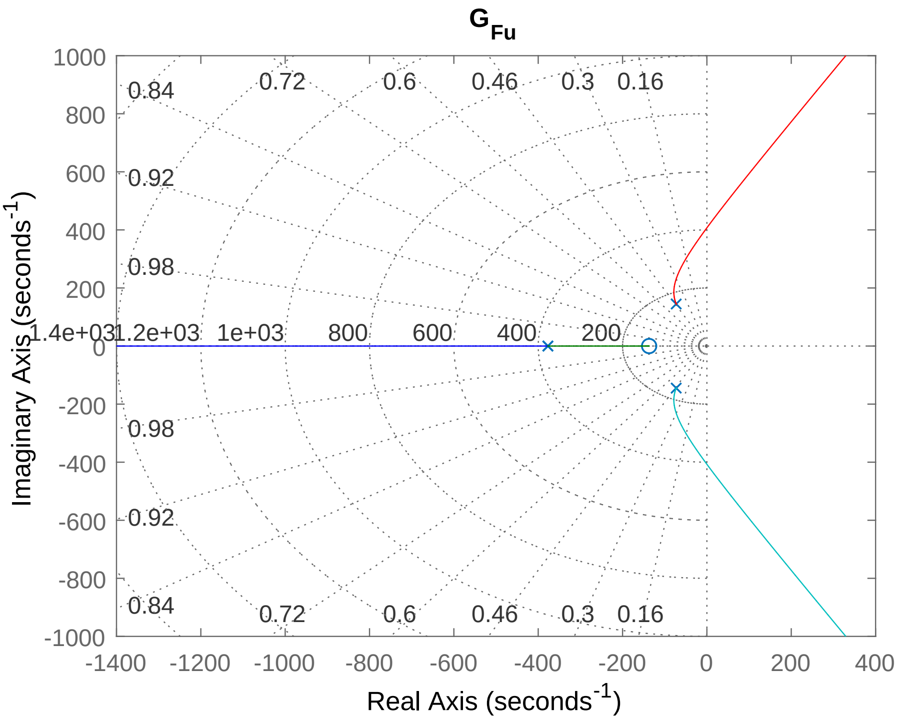

Figure 5.5. Root locus for the valve signal to load force system.

Before designing a controller to the system the accuracy of the linear model is investigated to determine if a controller designed from the linear model may be applicable in the non linear model.

5.1.3 Validation of Linear Model

To investigate if the derived linear model sufficiently depicts the non linear model the response of the two models are compared for a valve signal step of 10 %. As the valve dynamic was found to influence the system in the previous section the validation will be of the linear model including the valve dynamic as described by transfer function 5.8. The response of the two models is seen in Figure 5.6.

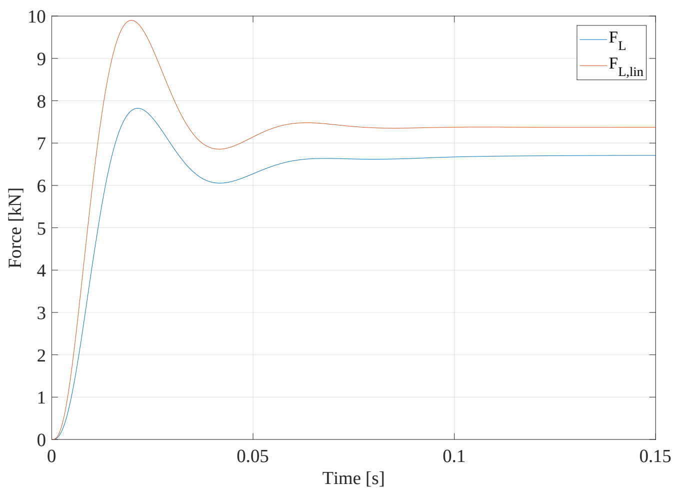

Figure 5.6. Linear and non linear model step response for a valve signal of 10%.

From the figure it can be seen that the response show coherence however the linear model seems to be less damped as it rises faster and with an overshoot of approximately 35 % while the non linear model has an overshoot of approximately 20 %. Both responses oscillate and have a settling time of approximately 60 ms. The non linear model reaches steady state at a load force of 6.7 kN while the linear model reaches a steady state load force of 7.4 kN resulting in a steady state error on the load force of 0.7 kN.

When linearising the model some simplifications were made so it is expected to see a linear model response that deviates from that of the non linear model to some extent. It is not known what exact simplification that leads to the steady state load force error. However the linear step response is concluded to mimic that of the non linear model fairly well and it is concluded that a force controller may be designed from the linear model.

Parameter study of soft parameters

As stated in the validation of the non linear model in Chapter 4 the friction force and the bulk modulus are soft parameters and their exact magnitudes are uncertain. From the validation of the model the soft parameters were given the values listed in table 4.2. As the Coulomb and Stribeck friction components were neglected due to non linearity the only friction force component in the linear model is the viscous damping. This leaves the linear model with the viscous damping coefficient and the bulk modulus as the only soft parameters which were given the values 100 kNs/m and 8000 bar, respectively. To investigate the impact of these parameters in the system a frequency response analysis is conducted for different damping and bulk modulus values. The bode plot for varying bulk modulus and varying viscous damping can be seen in Figure 5.7 and Figure 5.8, respectively.

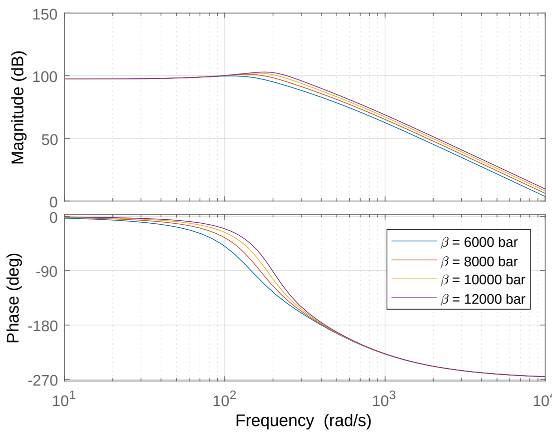

Figure 5.7. Bode plot for varying bulk modulus.

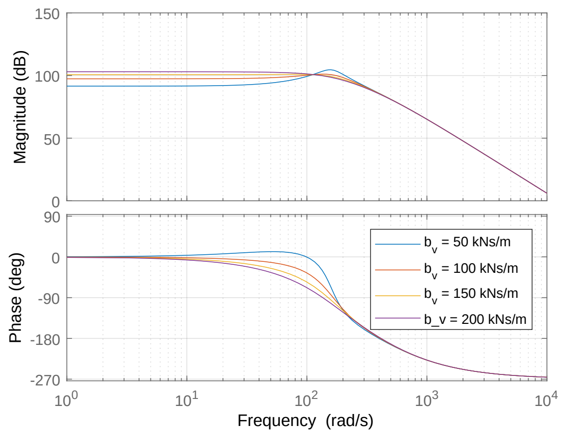

Figure 5.8. Bode plot for varying system damping.

From Figure 5.7 it is seen that at low frequencies the gain does not change when varying the bulk modulus. Around the breakaway frequency it is seen that increasing the bulk modulus results in a resonance peak indicating a lesser damped system. Furthermore the phase is seen to begin lagging sooner when lowering the bulk modulus. As the resonance peak has only slightly increased even at a bulk modulus of 12000 bar it is assumed that the error due to using a constant bulk modulus is small. It may be taken into consideration when designing a controller by designing it robust rather than aggressive.

From Figure 5.8 it is seen that the system gain increases when increasing the damping while reducing the resonance peak. By reducing the damping the gain decreases but in return the resonance peak is seen to increase. When lowering the damping the zero in the system transfer function is seen to contribute more as the phase starts to break away towards a phase shift of 90° before being dragged down by the poles. As the magnitude of the damping in the system is uncertain it will still be chosen as 100 kNs/m but when designing a controller it will be taken into account by valuing robustness over performance.

5.1.4 Controller Design

The initial approach for the controller design is to design a proportional controller. The control law for this is seen in Equation 5.11.

$$u_{\mathrm{v}} = k_{\mathrm{p}} F_{\mathrm{L,err}} \tag{5.11}$$

The proportional gain may now be chosen. It could be chosen as 5.5e-5 resulting in a marginally stable system as seen from Figure 5.5. However the system behaviour changes with the linearisation point as seen from the system bode plot (5.4) and the system may quickly become unstable. The step response for the closed loop system is shown in Figure 5.9 for three different proportional controllers. It is seen that a steady state error is present for all three proportional gains. The error is reduced when increasing the proportional gain but the response starts to oscillate more.

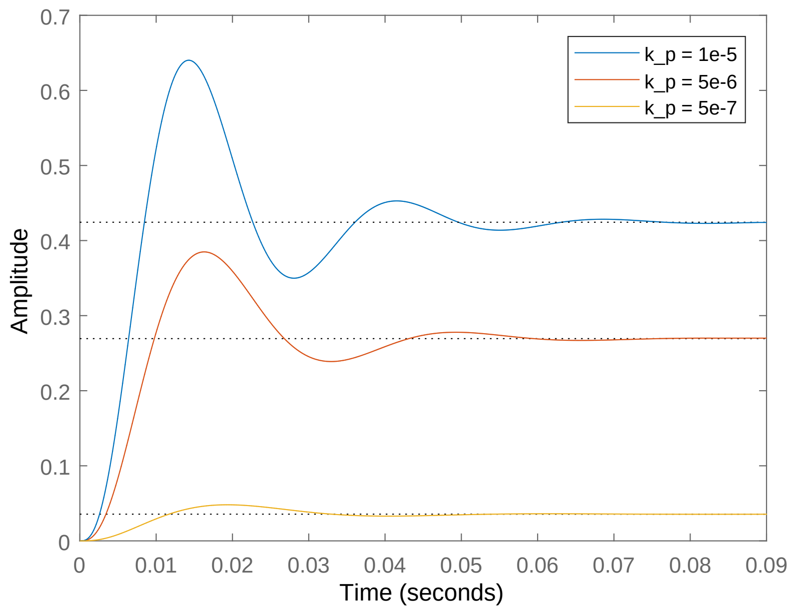

Figure 5.9. Step response for the closed loop system with different proportional controllers.

It is desired to design a controller capable of operating in the entire range of piston positions rather than a slightly faster controller only capable of operating in between certain points. For this reason a small proportional gain is chosen. However the steady state error should be eliminated so that the force applied by the cylinder will equal the reference force given. To eliminate the steady state error a PI controller is considered thereby adding an integrator to the controller. Instead of calculating an estimated integral gain which will most likely need to be tuned anyway the SISOtool in Matlab is employed. The SISOtool lets the user vary the bandwidth and phase margin so that a desired P,PI or PID controller is achieved for the linear model. From this approach a PI controller is chosen. The controller is on the form seen in Equation 5.12 with the gains listed in Table 5.2. Back calculation anti windup is implemented to prevent integrator windup.

$$G_{\mathrm{c}} = \frac{k_{\mathrm{p}} s + k_{\mathrm{i}}}{s} \tag{5.12}$$

Gain	Value
k_{p}	$6.5 \cdot 10^{-6}$
k_{i}	$9.8 \cdot 10^{-4}$

Table 5.2. PI controller gains.

5.1.5 Controller Performance in Non Linear Model

The controller is implemented in the non linear model and the performance is now tested for various step input of increasing magnitude. The reason for stepping in both directions is to investigate if the controller works in both directions as it was designed from a linear model corresponding to positive valve position. Figure 5.10 shows the tracking performance of the controller along with the force error and the normalised valve signal and valve spool position.

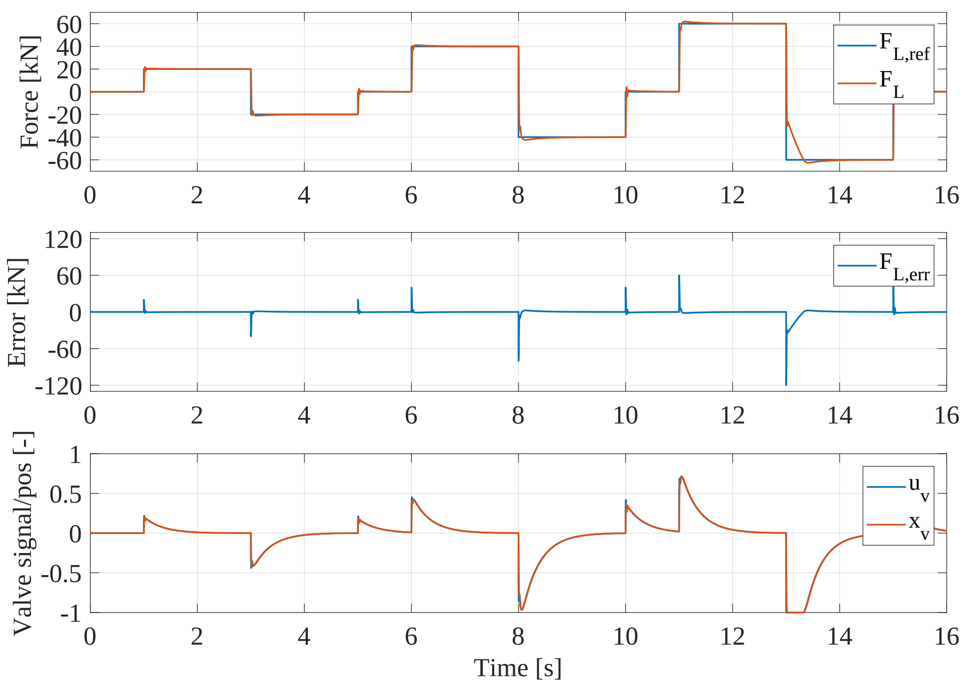

Figure 5.10. Step response of various magnitudes of the non linear model with the developed PI controller.

At steps of 20 and 40 kN the force is seen to track the reference well for both positive and negative steps and it is concluded that the developed controller works in both directions. At a negative step of 60 kN it can be seen that the force can not keep up with the reference. As the valve spool position is seen to have reached its limit the valve is fully open indicating that the force lagging the reference is a result of the time it takes to build up the pressure.

As a step input is given instantaneous it pressures the controller which is beneficial for ensuring robust and stable controller performance. The step response is however analysed solely to investigate the controller performance since it is rarely desired to apply forces in steps to a test object but rather in some constantly moving pattern such as a sine wave. The HALT test bench applies forces with a sine wave trajectory with a frequency of 0.5 Hz. The controller performance for a sinusoidal load force reference is seen in Figure 5.11. The reference has a magnitude of 30 kN and a frequency of 1 Hz.

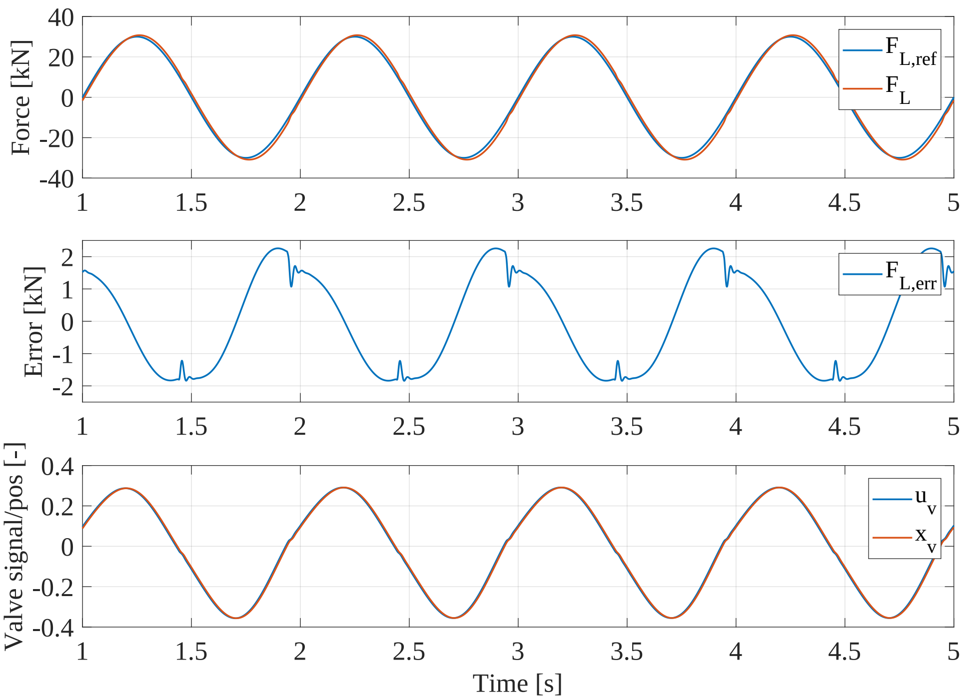

Figure 5.11. Response of the non linear model with the developed PI controller following a sinusoidal reference.

From the figure it can be seen that the force show good coherence with the reference while good coherence is also seen between the normalised valve signal and the valve spool position. The force is however slightly phase shifted resulting in a error on the force varying between -1.9 and 2.2 kN with a mean error of 1.3 kN. The error is seen to oscillate when it is around its maximum magnitude which is when the force crosses zero. The oscillations happen when the force becomes sufficiently small and can not overcome the Stribeck friction. This slows down the piston and the velocity is decreased which increases the friction further. As the force again increases the friction is overcome which is why the oscillations occur only when the force is small.

The performance of the controller designed in this chapter is used for evaluating an extended control structure including a valve compensator designed in the following chapter.

Compensator Design 6

This chapter contains design of a valve compensator and implementation of this into the control structure. Furthermore the performance of the compensator is evaluated.

6.1 Valve Compensator

To compensate for some of the non linear behaviour in the valve the control structure may be extended by employing a valve compensator as illustrated in Figure 6.1. The valve has been separated from the system since it is assumed to be cancelled out by the compensator. Furthermore it allows for a definition of a system plant taking the piston side flow as input and providing a force.

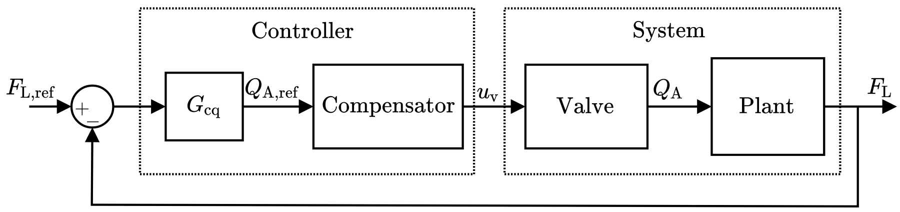

Figure 6.1. Control structure including controller and compensator.

The concept of a valve compensator is to make use of knowledge of the valve behaviour to eliminate some of the non linearity in the system. The valve signal is the only input that is controlled in the system and as it is described by the non linear orifice equation, it is beneficial to compensate for some of the non linear behaviour since it may yield a more robust control structure.

The flow through the valve is described by the orifice equation as formulated in Chapter 4 Equation 4.7 and depends on the valve spool position x_v, the valve constant k_v and the pressure difference across it Δp. As the pressures in the system are measured the pressure drop across the valve may be calculated. Using the pressure drop and the valve constant given by the datasheet MOOG [2009] it is possible to formulate a control law for the compensator by inverting the orifice equation formulated for the valve flow which then calculates a valve spool position corresponding to a desired flow as formulated in Equation 6.1.

$$u_v = Q_{A,ref}\frac{1}{k_{vC}}\begin{cases}\frac{1}{\sqrt{p_S - p_A}}\ , & \text{for } x_v \geq 0\\ \frac{1}{\sqrt{p_A - p_T}}\ , & \text{for } x_v < 0\end{cases} \tag{6.1}$$

If the valve is ideal the compensator valve constant k_{vC} equals the valve constant k_v and the compensator cancels out the valve behaviour except for the valve spool dynamic. As the valve constant is an empirically determined parameter it is however unlikely that it depicts the valve perfectly and by distinguishing between it and the compensator valve constant it is possible to make up for potential uncertainties affecting the flow by adjusting the compensator valve constant. This concept is illustrated in Figure 6.2 where the control law for the compensator has been employed.

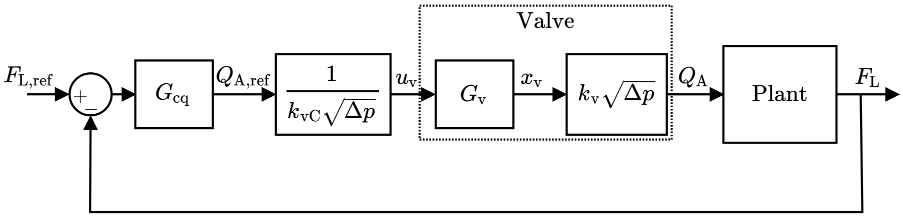

Figure 6.2. Control structure including valve compensator.

From the figure it is obvious that if $k_{vC} = k_v$ the compensator cancels out the valve gain and the only difference between the reference flow and the actual flow is the valve spool dynamic.

6.1.1 Load Pressure Compensating

Recall that the valve flow was expressed as a function of the load pressure when the reduced order model was derived in section 4.2. This expression may be inverted in the same manner as described above to form a slightly different control law for the compensator as seen in Equation 6.2.

$$u_v = Q_{A,ref}\frac{\sqrt{\sigma^2+\alpha^3}}{k_{vC}\sigma}\begin{cases}\frac{1}{\sqrt{p_S-p_L-\alpha p_T}} & \text{, for } x_v \geq 0\\ \frac{1}{\sqrt{\alpha p_S+p_L-p_T}} & \text{, for } x_v < 0\end{cases} \tag{6.2}$$

The main difference from the first compensator is that this compensator depends on the load pressure and thereby depend on both the piston side chamber pressure and the rod side chamber pressure while the first compensator depends only on the piston side chamber pressure.

6.2 Frequency Response Analysis

As suggested above the valve gain is cancelled out by the compensator. To design a controller to the remaining system a frequency response analysis of the system with the piston side flow as input is conducted in the following. Whether the system should take the reference flow or the actual flow as input depends on if the valve dynamic is included in the system. It is not yet known if it is necessary to include the valve dynamic but it will be investigated along with the following frequency response analysis. Figure 6.3 shows a block diagram of the linear model with the valve flow as input. Note that the valve dynamic is not included.

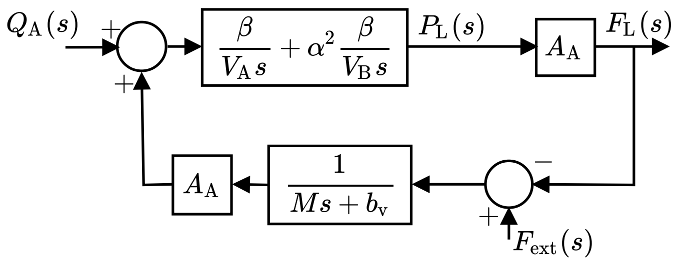

Figure 6.3. Block diagram of the linear model with piston side chamber flow as input.

By substituting the expression for the piston position (5.2) into the expression for the load pressure (5.3) and isolating for the load pressure it may be expressed as:

$$P_L(s) = \frac{C_H(Ms + b_v)Q_A(s) + C_H A_A F_{ext}(s)}{Ms^2 + b_v s + C_H A_A^2} \tag{6.3}$$

From the load force definition (5.1) the load force system may be formulated as

$$F_L(s) = \frac{A_A C_H(Ms + b_v)Q_A(s) + C_H A_A^2 F_{ext}(s)}{Ms^2 + b_v s + C_H A_A^2} \tag{6.4}$$

From the transfer function (6.4) it can be seen that the load force depends on two inputs, which are the piston side flow $Q_A(s)$ and the external force acting on the piston $F_{ext}(s)$. However only one input is permitted in transfer function analysis. By describing the external force $F_{ext}(s)$ as a disturbance in the system it is neglected and the transfer function from piston side flow to load force may be formulated as:

$$G_{Fq}(s) = \frac{F_L(s)}{Q_A(s)} = \frac{A_A C_H(Ms + b_v)}{Ms^2 + b_v s + C_H A_A^2} \tag{6.5}$$

The valve and valve compensator is not included in the system as the compensator is assumed to cancel out the valve gain. The valve dynamic is however still part of the system. By including it in the system the transfer function for the reference flow to load force system is described as:

$$G_{Fqref}(s) = \frac{F_L(s)}{Q_{A,ref}(s)} = G_v(s)\frac{F_L(s)}{Q_A(s)} = \frac{\omega_n^2}{s^2 + 2\zeta_v\omega_n s + \omega_n^2}\frac{A_A C_H(Ms + b_v)}{Ms^2 + b_v s + C_H A_A^2} \tag{6.6}$$

The transfer function is not normalised as it is clearly seen that it yields a transfer function on a form similar to that of the valve signal to load force system as described by Equation 5.8 with a denominator of fourth order and a zero in the numerator. The reference flow to force system is compared to the flow to force system in the bode plot seen in Figure 6.4 using the system values listed in Table 5.1.

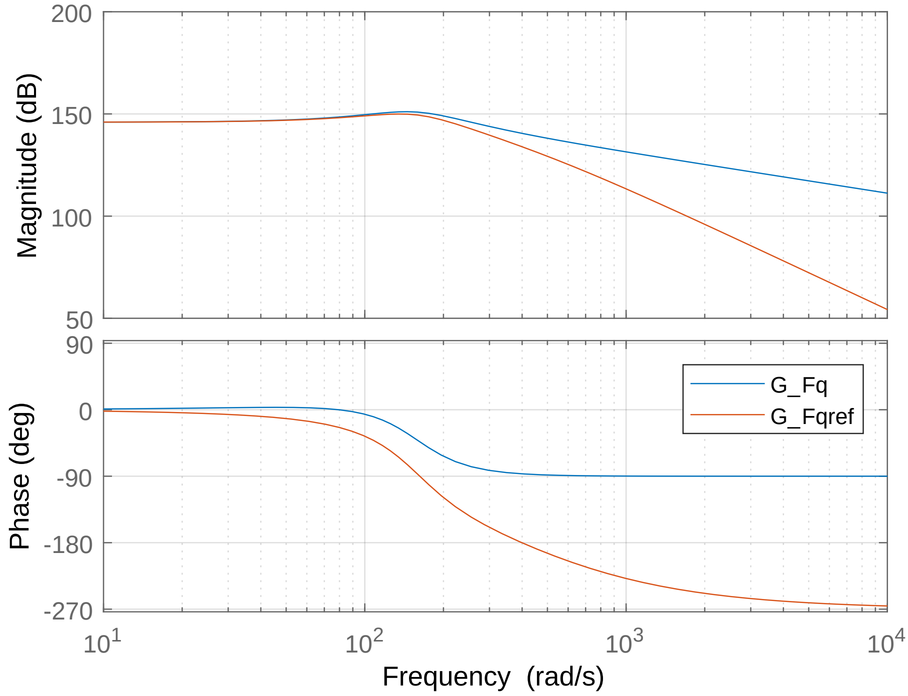

Figure 6.4. Bode plot for the load force system with the flow Q_A and flow reference $Q_\mathrm{A,ref}$ as input, respectively.

The bode plot for the reference flow to force system differs from the flow to force system in the same manner as that of the valve signal to force system was found to differ from the valve spool position to load force system. However the magnitude of the gain is approximately 45 dB greater for the flow to force systems. Furthermore closed loop instability is indicated for the reference flow to force system as the gain margin is negative. The controller will therefore by designed from the reference flow to force system as described by Equation 6.6.

6.2.1 Flow Controller Design

The flow controller G_cq is designed by closing the loop in the reference flow to force system and using SISOtool to tune the controller. This resulted in a PI controller on the form seen in Equation 5.12 with the gains listed in Table 6.1.

Gain	Value
k_p	$7.3 \cdot 10^{-8}$
k_i	$7.1 \cdot 10^{-6}$

Table 6.1. PI controller gains for G_cq.

The magnitude of the gains may be evaluated by recalling that the controller takes the error of the force as input and delivers a reference flow as output. The unit of the gains is thereby $\frac{\mathrm{m^3/s}}{\mathrm{N}}$ and as the force error may be in the range of kN while the reference flow may be in the range of 50 l/min which corresponds to a flow of approximately $8 \cdot 10^{-4}\,\frac{\mathrm{m^3}}{\mathrm{s}}$ it seems reasonable that the gains should be of small magnitude.

6.3 Controller Performance in Non Linear Model

The full controller consisting of the flow controller G_{cq} and the compensator may now be tested in the non linear model. First the performance of the controller is tested by assuming ideal valve flow conditions. As mentioned in the previous section this implies that the valve compensator cancels out the valve gain following directly from the assumption that $k_{vC} = k_v$. The valve dynamic is not compensated for and thus not cancelled out but it is assumed that it is sufficiently faster than the system and does not influence the system significantly.

To investigate the performance of the two compensators formulated above they are implemented in the non linear model and given a sinusoidal load force reference and their tracking performance are seen in Figure 6.5. The compensator compensating based on the piston side pressure and the compensator compensating based on the load pressure are denoted compensator 1 and compensator 2, respectively.

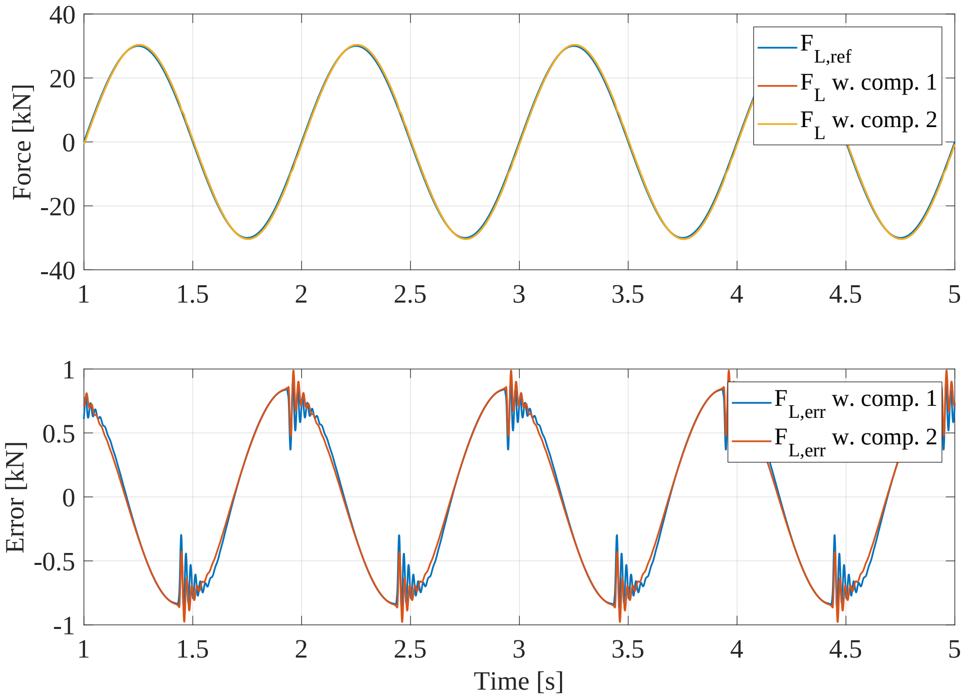

Figure 6.5. Comparison of the performance of compensator 1 and 2.

From the figure the force is seen to be tracking the reference well yet the error reaches a maximum value of approximately 0.9 kN for compensator 1 and approximately 1 kN for compensator 2. The error is seen to oscillate slightly less at low velocities using compensator 2. The mean error are found to be 533 N for compensator 1 and 537 N for compensator 2 suggesting that the best tracking performance is achieved when compensating using only the piston side pressure and not the load pressure. Nevertheless the compensators are seen to have somewhat similar performance. The error is seen to oscillate when it is around its maximum magnitude which is when the force crosses zero. As suggested also when evaluating the force controller in Chapter 5 the oscillations happen when the force becomes sufficiently small and can not overcome the Stribeck friction. This slows down the piston and the velocity is decreased which increases the friction further.

As the force again increases the friction is overcome which is why the oscillations occur only when the force is small.

The ability of the two compensators to estimate the flow are evaluated in Figure 6.6 where the actual piston side flow is plotted against the reference piston side flow given by the PI controller. Compensator 1 is seen to estimate the flow well however with a mean error of 1.2 l/min. The sinusoidally varying error indicates that the error is primarily related to a small phase shift which is caused by the valve dynamic. Compensator 2 is seen to estimate the flow fairly well but as the piston velocity becomes low and oscillations occur the error is seen to break away and reach approximately 5.5 l/min before settling. Despite this error on the flow the desired actual flow is still achieved as the PI controller adjusts the reference flow accordingly.

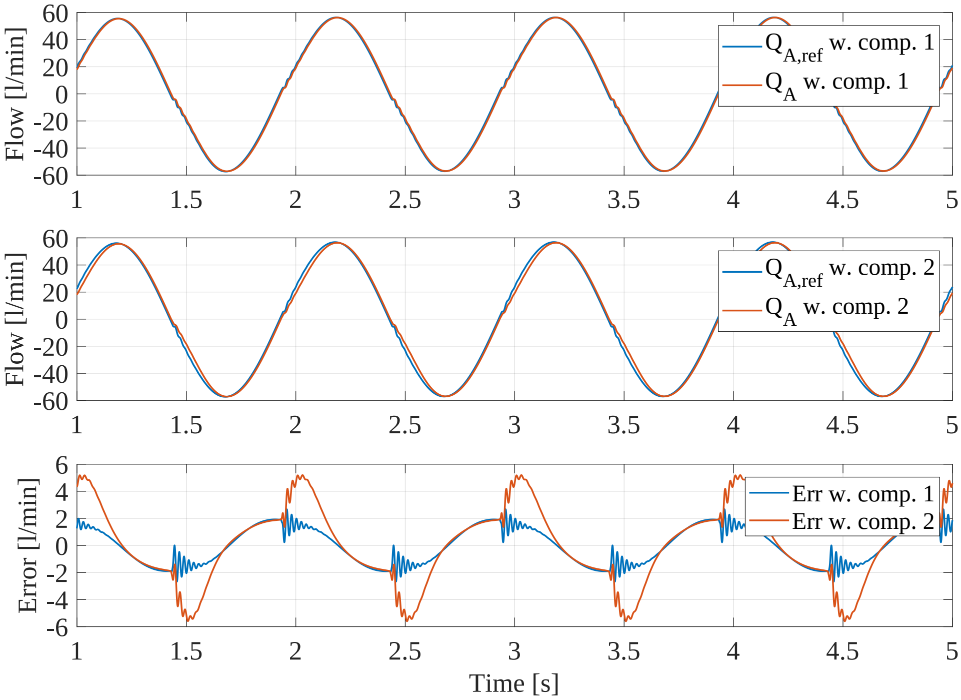

Figure 6.6. Comparison of the flow estimation performance of compensator 1 and 2.

Even though the two compensators show similar performance in tracking the force it is preferred to have a compensator that cancels out the valve gain as good as possible so that the controller characteristic is primarily determined by how the PI controller is designed. To cancel out the valve gain the valve flow estimation should be as good as possible and as the better flow estimation is achieved with compensator 1 it is chosen as the superior solution for the case of controlling the flow in and out of the piston side chamber.

6.3.1 Comparison of Controller Performance

To compare the performance of the full controller with the two compensators to the controller designed in Chapter 5 their performance are plotted together in Figure 6.7.

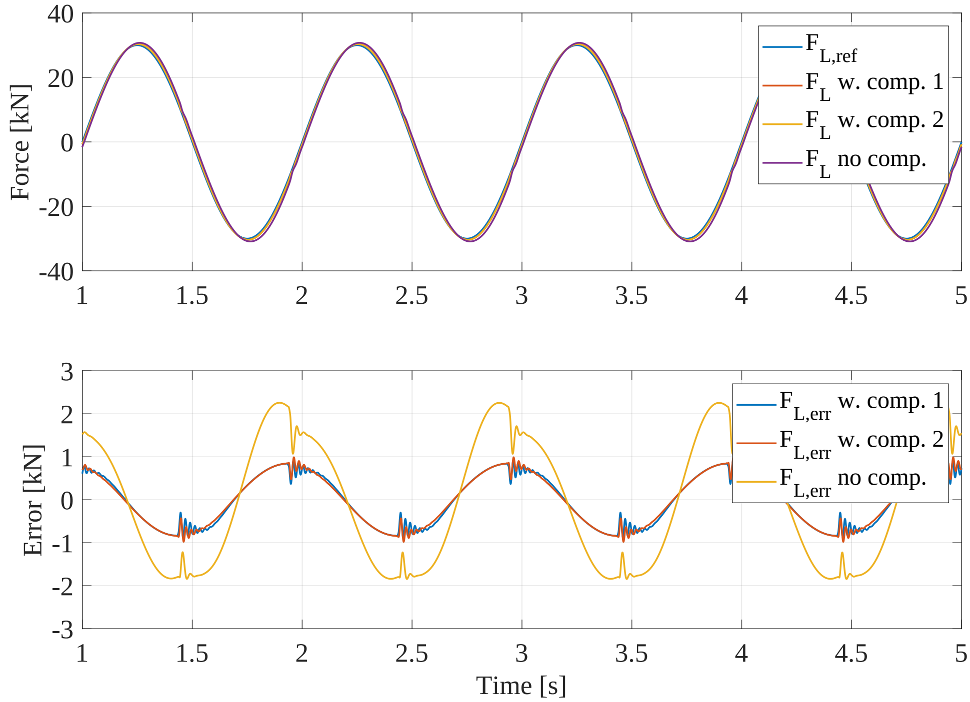

Figure 6.7. Comparison of the performance of compensator 1, compensator 2 and no compensator.

When plotted together it is clear to see that the performance of the controller without compensator is quite similar to that of the controller including a compensator. As the mean error of the controller without compensator was found to be 1311 N while it for the controller with compensator 1 was found to be 533 N the deviation from the reference for the two controllers are 4.4 % and 1.7 %, respectively. The error of the controller without compensator is thereby more than twice as large as when employing the compensator. This issue may however be related to the design of the PI controllers rather than to the effect of the compensation as the PI controller with the compensators may be a bit more aggressive. This would also explain why the error on the force is oscillating more at small force magnitudes compared to the performance of the controller without compensator. It should be mentioned that the error has the tendency of a sine wave and that it may be the system and not the controller that causes most of the error by phase shifting the force slightly. This suggests that the load force is actually following the reference but with a small phase shift.

Controller Performance when Varying Supply Pressure

As the compensator cancels out the valve gain the controller with compensator was designed based on a linear model which in terms of linearisation point depends only on the piston position. The controller without compensator was designed based on a linear model that contains a linear approximation of the orifice equation and thus depends on the linearisation point of both pressure, valve spool position and piston position.

To investigate the controller performance away from the linearisation point their performance are compared for a reduced supply pressure. The controller without compensator was designed based on a supply pressure of 250 bar. The controller with compensator was designed independent on the pressure as it is cancelled out by the compensator.

As the two compensators show similar performance only one of them is used for investigating the impact of varying the supply pressure. As compensator 1 was found to best estimate the flow it is the one used in the following analysis. The controller performance is seen in Figure 6.8 for a supply pressure of 100 bar, a reduction of 60 %.

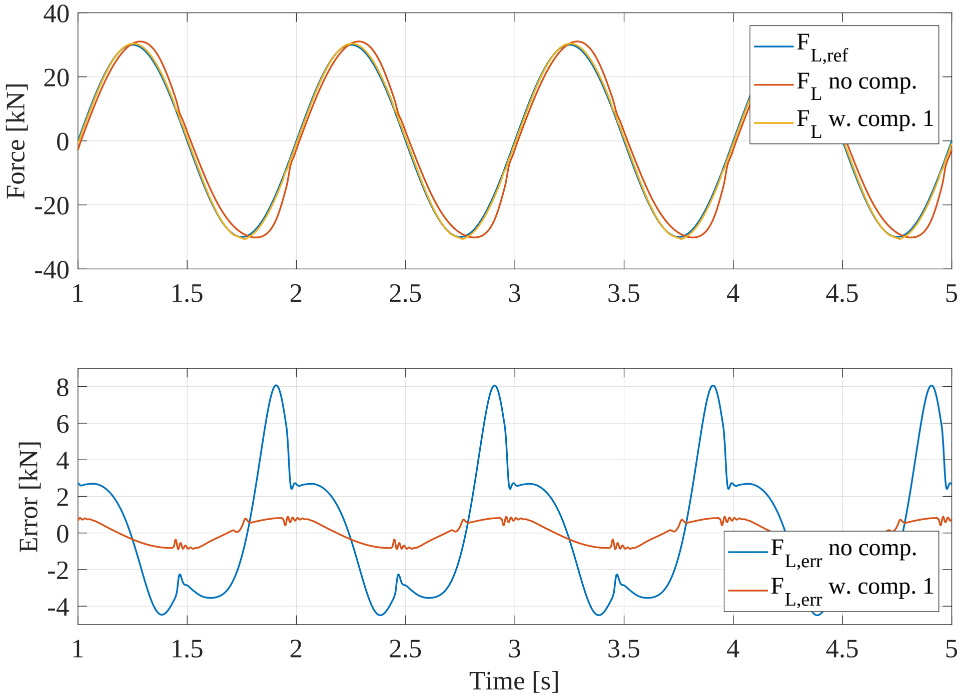

Figure 6.8. Comparison of the performance of the controller with and without compensator for a supply pressure of $p_S = 100$ bar.

From the figure it is seen that the force is phase shifted additionally and is also no longer a perfect sinus for the controller without compensator. This results in the error reaching 4.6 kN for piston movement in the negative direction and 8 kN for piston movement in the positive direction. The reason for the error being larger for piston movement in the positive direction is that the cylinder is asymmetrically constructed because a larger pressure increase thereby is necessary on the rod side to yield the same force due to the smaller area. The mean error is found to be 3098 N which is an increase of 136 % compared to the error of 1311 N at full supply pressure.

The performance of the controller with the compensator is seen handle the changed conditions well as the error remains close to unchanged with an mean error of 550 N which is an increase in error of 3 % compared to the error at full supply pressure. This relatively large difference in controller performance makes sense by recalling that as the system pressures is fed back into the compensator it can compensate for the lower supply pressure while the controller without compensator was designed at a linearisation point of a higher supply pressure and therefore designed to handle a different situation.

It is concluded that the controller performance around the linearisation point is slightly improved when employing a valve compensator. This may be an improvement induced by the compensator but it might also be related to slightly different tuning of the two PI controllers. As the supply pressure is lowered thereby moving the working point away from the linearisation point the controller with the compensator shows the best performance as the mean error is only increased by 3 % compared to the controller without compensator for which the mean error is increased by 136 %.

6.3.2 Robustness of Compensator

The above analysis is based on the assumption that the compensator cancels out the valve gain, that is $k_{\mathrm{vC}} = k_{\mathrm{v}}$, and the only remaining influence from the valve is the dynamic and a small uncertainty in pressure measurements. In practice this is probably rarely the case and so the compensator constant k_{vC} may be adjusted slightly so that a desired flow is achieved. It is however uncertain how it affects the system when the compensator constant is changed. Figure 6.9 shows the influence on the force when decreasing the compensator constant while Figure 6.10 shows the influence on the force when increasing the compensator constant.

From the figures it is seen that decreasing the compensator constant below $0.5k_{\mathrm{vC}}$ will lead to an unstable system. When increasing the compensator constant the force is seen to be phase shifted. There is however nothing that indicates instability for an increased compensator constant.

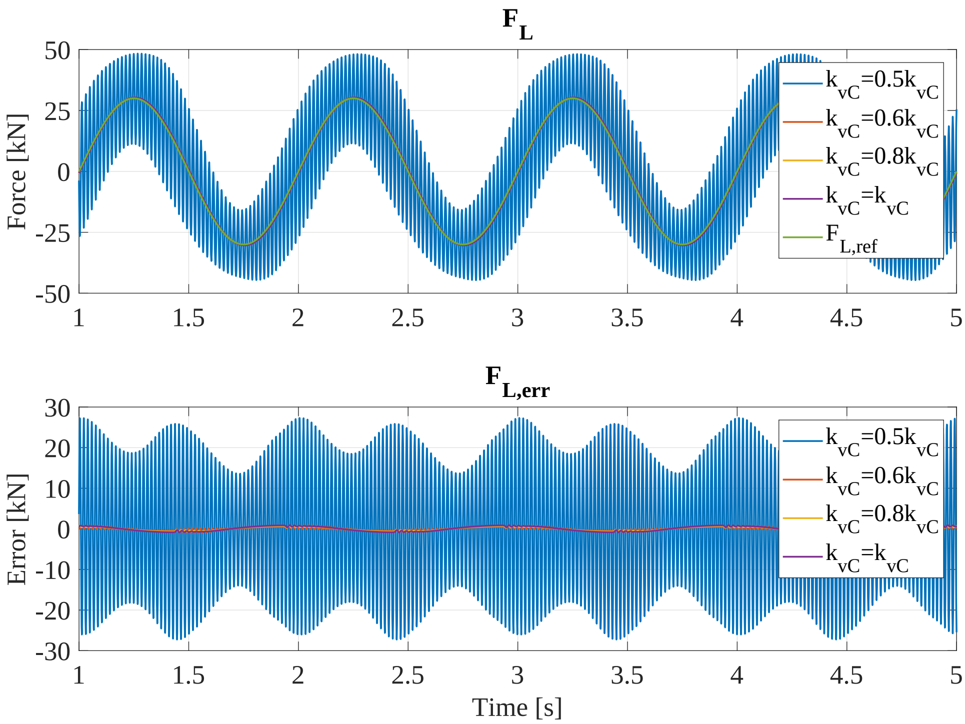

Figure 6.9. Effect of decreasing the compensator constant k_{vC} for compensator 1.

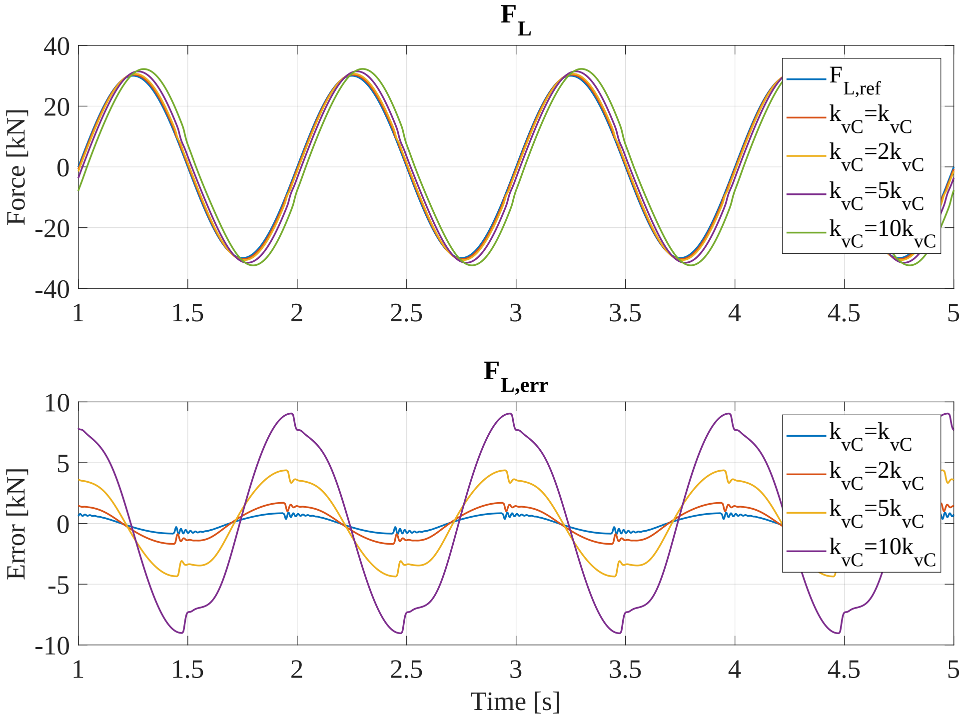

Figure 6.10. Effect of increasing the compensator constant k_{vC} for compensator 1.

The effect of changing the compensator constant may be investigated by analysing how it affects the gain of the full controller. By inspecting the compensator formulation in Equation 6.2 it is seen that the compensator constant is inverse proportional to the gain of the controller. The proportional gain of the full controller is then increased when the compensator constant is decreased and vica versa. By inspecting Figure 6.9 and Figure 6.10 the system behaviour is seen to correspond to this relationship. Decreasing the compensator constant does result in a higher gain and thereby a more aggressive controller and for a compensator constant decrease of both 20 % and 40 % the error is actually seen to be reduced slightly. As the constant is reduced by 50 % the controller becomes too aggressive and the system becomes unstable. As the constant is increased an increased phase shift is seen while the magnitude of the force is seen to overshoot the reference slightly. The phase shift and overshoot is increased as the compensator constant is increased but even when increasing the constant 30 times there is no sign of the system becoming unstable. This makes sense as it is equivalent to decreasing the proportional gain of the controller thereby making it slower and more robust.

From the above it may be concluded that an estimate of the valve constant may be used as compensator constant when designing a valve compensator since the exact value is not important. The compensator constant should however be estimated with respect to the formulated flow controller. If the flow controller is already so aggressive that it is close to making the system unstable an estimate of the compensator constant should be performed carefully as if the estimate is too low compared to the actual value it may result in instability.

6.3.3 Compensating with Limited Feedback

The two compensators formulated in the above as seen in Equation 6.1 and Equation 6.2 depend on knowing the valve constant and the possibility of measuring the system pressures and the valve spool position. As concluded in the previous section the exact value of the valve constant is not needed but an estimate will do.

Compensating without Valve Position Feedback

A system is now considered where the valve spool position can not be measured. As the compensator was found to improve the controller performance it would still be desired to implement it in the system.

As seen from the formulation of the compensator in Equation 6.1 the measured valve spool position is used for determining which pressure drop should be used in the compensator as this changes when the valve spool position changes sign. As the valve spool position can not be measured it is suggested to instead use the valve signal u_v. This was found to yield satisfactory performance similar to the performance when using the valve spool position. This may however be a result of using a valve with fast dynamic. Using the valve signal as feedback to the compensator for a valve with slow spool dynamic may result in using a wrong pressure drop in the compensator as the valve signal may switch fast but the valve spool position takes time to switch as well. Using the valve signal as feedback to the compensator should therefore be performed carefully with respect to the valve dynamic.

Now consider a system where neither valve spool position nor valve signal can be measured. It is instead suggested that the force reference is fed to the compensator to determine which pressure difference to use in the compensation. This is suggested since when the sign of the force switches from positive to negative or vica versa the valve will presumably switch as well as the supply pressure should be used to build up the pressure in the opposite chamber. Then the control law for the compensator is formulated as seen in Equation 6.7 when compensating with respect to the piston side pressure and not the load pressure.

$$u_\mathrm{v} = Q_\mathrm{A,ref}\frac{1}{k_\mathrm{vC}}\begin{cases}\frac{1}{\sqrt{p_\mathrm{S}-p_\mathrm{A}}} & \text{, for } F_\mathrm{L,ref} \geq 0\\ \frac{1}{\sqrt{p_\mathrm{A}-p_\mathrm{T}}} & \text{, for } F_\mathrm{L,ref} < 0\end{cases} \tag{6.7}$$

The performance of the full controller with the compensator seen in Equation 6.7 is seen in Figure 6.11 compared to the performance of the original compensator formulation. The only difference between the two compensators is the variable governing which pressure drop to use for calculating the valve signal.

When the force reference is used for governing the compensator the mean error is 539 N which is only a 1 % increase compared to the error when the valve spool position is governing the compensator. However the error is seen to oscillate more with large spikes when the force changes from positive to negative. When the force crosses zero it switches sign and thereby switches the pressure drop used in the compensator. As the error spike happens just when the force crosses zero it is suspected that the switch in pressure drop is not happening at the correct time.

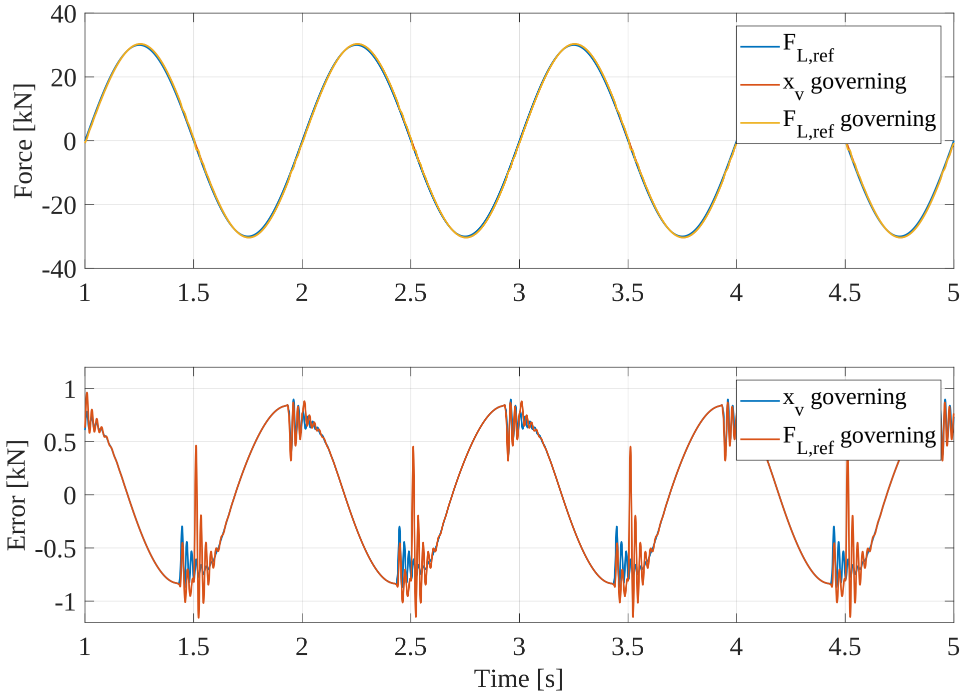

Figure 6.11. Comparison of the performance of compensator 1 with the valve spool position and the force reference governing the compensator, respectively.

To investigate this issue the valve spool position and the normalised force is plotted along with the switch signal that tells the compensator when to switch the pressure drops. This is seen in Figure 6.12 where the valve spool position is governing the compensator in the first plot and the force reference is governing the compensator in the second plot.

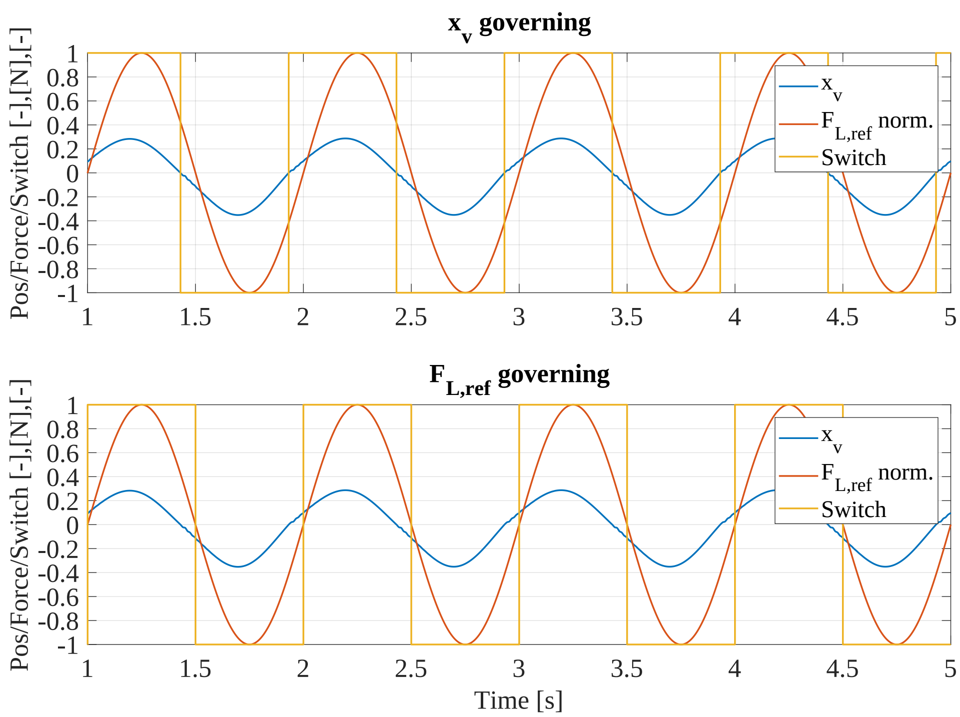

Figure 6.12. Comparison of compensator behaviour when the valve spool position is governing the control and when the force reference is governing the control, respectively.

From the figure it is seen that when the valve spool position governs the compensator the switch occurs exactly when the valve spool position crosses zero and changes sign. This results in the pressure drop used in the compensator is correct at all times meaning that as long the valve spool position is positive the pressure drop used in the compensator is $p_S - p_A$ while the moment the valve spool position switches to negative the pressure drop used will be $p_A - p_T$. When the force reference is governing the compensator the switch is seen to occur when the valve spool position has already changed sign and opened approximately 10 % to the opposite side. This is due to a phase shift between the force and the valve spool position. This results in an incorrect pressure drop being used in the compensator for the first 80 ms after each sign switch of the valve spool position. Then the force reference crosses zero and corrects the pressure drop in the compensator. This delayed switch causes the spike in the error seen in Figure 6.12.

Compensating without Pressure Feedback

Now a system is considered where the valve spool position is measured but the pressures are not. As the pressures are not measured they can not be fed to the compensator. Instead a fixed value for the pressure drop is used in the compensator. Figure 6.13 shows the performance of the controller and compensator when the compensator is fed various constant supply pressures compared to the performance when the actual pressure drop is used. When given the used load force trajectory and the actual pressure is fed to the compensator the mean pressure in the piston side chamber is 105 bar. From the figure it is seen that the when the compensator is given a constant pressure drop the controller still manages to track the force reference fairly well. The oscillations in the error are seen to increase especially for a constant pressure of 50 bar and 150 bar which is the constant pressures used which is farthest from the actual mean pressure.

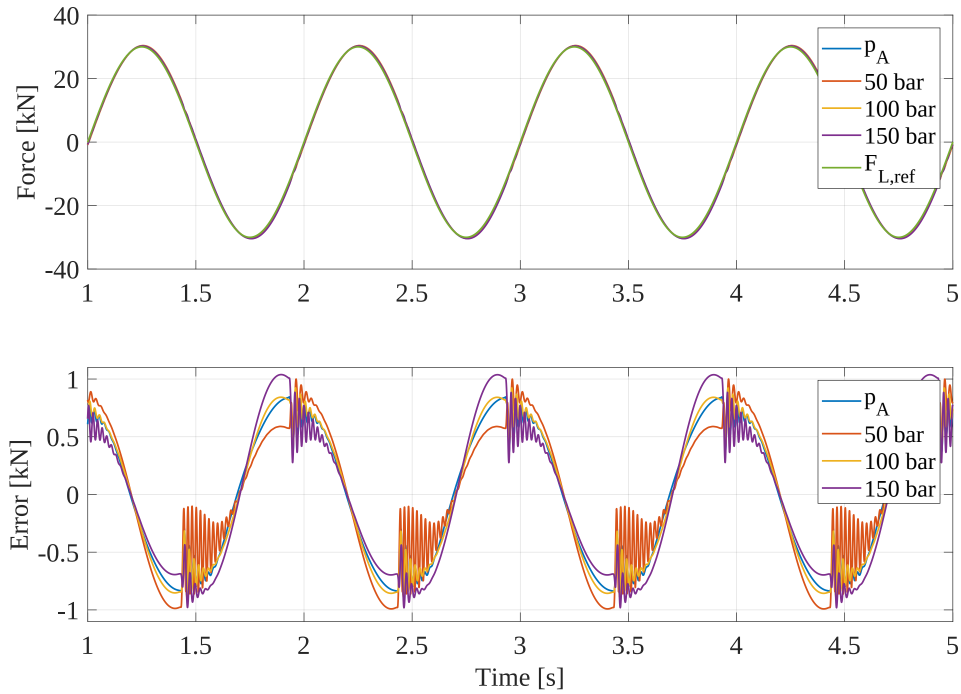

Figure 6.13. Comparison of compensator performance when a constant pressure is used instead of actual pressure feedback.

Why the full controller keeps tracking the force reference even though the compensator is using a wrong pressure drop for calculating the valve signal may be investigated by looking at the piston side flow. Figure 6.14 shows the piston side flow for the different compensators used in Figure 6.13 and the corresponding reference flow.

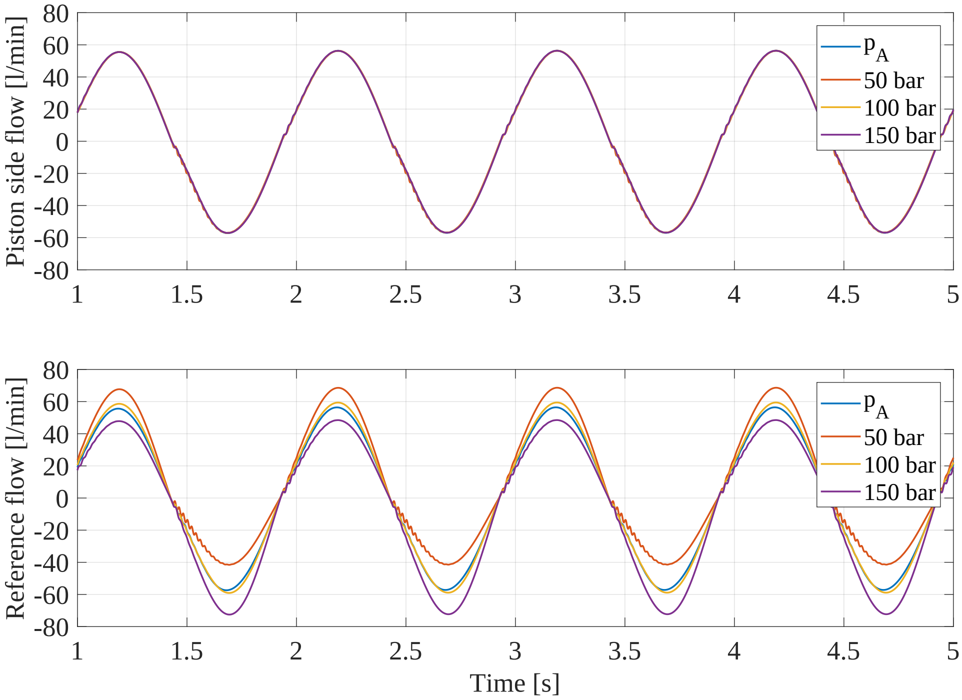

Figure 6.14. Comparison of flow and reference flow when a constant pressure is used instead of actual pressure feedback.

From the figure it is seen that the flow is approximately the same for all compensators. The flow reference is however seen to change when changing the used compensator pressure. The reason for the full controller being able to track the force reference for all the compensators is because the PI controller changes the reference flow accordingly so that the correct actual flow is achieved.

It is concluded that if the system in question is to maintain close to constant pressure levels a compensator without pressure feedback may be employed. In such a scenario it is however possible that a compensator is not needed as the valve is not to be controlled much anyway. When dealing with a system where the pressure levels are to be varied within a large scale it is proposed that a compensator with pressure feedback is employed as the compensator performance is compromised when the actual pressure differs a lot from the pressure used in the compensator. Furthermore it may increase oscillations or discontinuities as indicated by Figure 6.13 potentially leading to instability.

Matching Valve to Actuator Analysis 7

In the previous chapter it was found that the valve compensator is dependent on the pressure drop across the valve. The cylinders in the test setup are controlled by symmetrical valves. That is valves where the flowpath areas are designed symmetrically and are thereby equal i.e. $A_{\mathrm{BT}} = A_{\mathrm{SA}}$ and $A_{\mathrm{SB}} = A_{\mathrm{AT}}$ where the subscript denotes the flowpath with S,T,A,B being supply, tank, piston side chamber and rod side chamber, respectively. Using a symmetrical valve to control an asymmetrical cylinder will result in the pressure drop across the two flowpaths to be of unequal magnitude as the pressure drops depend on the flow through the valve as seen from the orifice equation in Equation 4.4. It is however possible to construct the valves so that the pressure drop across the two flowpaths becomes equal.

7.1 Matching Valve to Actuator Ratio

By isolating for the pressure drop in the orifice equations for the flows through the valve the pressure drops for a positive valve spool position are found to be

$$\Delta p_{\mathrm{SA}} = \frac{\rho}{2}\frac{Q_{\mathrm{A}}^2}{C_{\mathrm{d}}^2 A_{\mathrm{SA}}^2} \qquad \Delta p_{\mathrm{BT}} = \frac{\rho}{2}\frac{Q_{\mathrm{B}}^2}{C_{\mathrm{d}}^2 A_{\mathrm{BT}}^2} \tag{7.1}$$

Now recall that when assuming steady state flow conditions the rod side flow may be expressed as $Q_{\mathrm{B}} = \alpha Q_{\mathrm{A}}$. Substituting this into the expression for the pressure drop yields

$$\Delta p_{\mathrm{BT}} = \frac{\rho}{2}\frac{(\alpha Q_{\mathrm{A}})^2}{C_{\mathrm{d}}^2 A_{\mathrm{BT}}^2} \tag{7.2}$$

From Equation 7.2 it is seen that the flow path areas and the area ratio squared distinguishes the two pressure drops. By changing the flow path area so that $A_{\mathrm{BT}} = \alpha A_{\mathrm{SA}}$ the pressure drops are found to be equal as

$$\Delta p_{\mathrm{BT}} = \frac{\rho}{2}\frac{(\alpha Q_{\mathrm{A}})^2}{C_{\mathrm{d}}^2 (\alpha A_{\mathrm{SA}})^2} = \frac{\rho}{2}\frac{Q_{\mathrm{A}}^2}{C_{\mathrm{d}}^2 A_{\mathrm{SA}}^2} = \Delta p_{\mathrm{SA}} \tag{7.3}$$

The pressure drops across the two flowpaths are thereby found to be equal when the relationship between the flowpath areas is $A_{\mathrm{BT}} = \alpha A_{\mathrm{SA}}$ or similarly $k_{\mathrm{vB}} = \alpha k_{\mathrm{vA}}$.

7.2 Controller Performance using a Matched Valve

To investigate the controller performance when using a matched valve the current system model is changed so that $k_{\mathrm{vB}} = \alpha k_{\mathrm{vA}}$. This is the only thing that is changed in the system model for performing the following analysis. Note that the valve now used in the model is different from the valve in the test setup where $k_{\mathrm{vA}} = k_{\mathrm{vB}} = k_{\mathrm{v}}$.

As the model has been changed the derived linear model changes as well as the flowpath ratio is changed from 1 for the symmetrical valve to $\sigma = \frac{k_{\mathrm{vB}}}{k_{\mathrm{vA}}} = 0.75$ for the matched valve. As seen from the linear model in Equations 4.53 to 4.55 the expression for the flow is the only expression dependent on σ and since the flow was used as input when designing the flow controller (G_{cq}) this controller may as well be employed in the system with the matched valve. Compensation with respect to the piston side chamber pressure (compensator 1) is used for estimating the valve signal. The previously used force trajectory is now used as reference in the model and the performance is plotted along with the performance of the original system as seen in Figure 7.1.

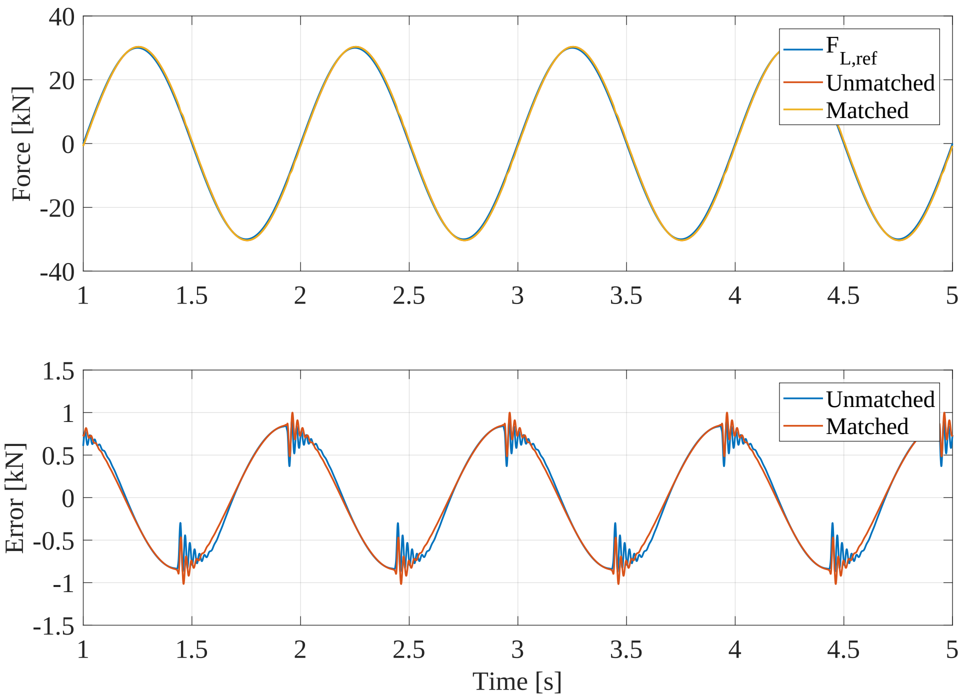

Figure 7.1. Comparison of force tracking performance with an unmatched and a matched valve.

When using a matched valve the force tracking performance is seen to be approximately equal to that of the unmatched. The mean error for the system with the unmatched valve is as mentioned earlier 533 N while the mean error for the system with the matched valve is 537 N. To investigate the effect of employing a matched valve on the pressure drops across the valve they are plotted in Figure 7.2 for both systems. For the original system using the unmatched valve the pressure drop in the A-line is seen to range between 80 - 155 bar while the pressure drop in the B-line is seen to range between 50 - 180 bar. For the system using a matched valve the two pressure drops are seen to be approximately equal both ranging between 70 - 160 bar.

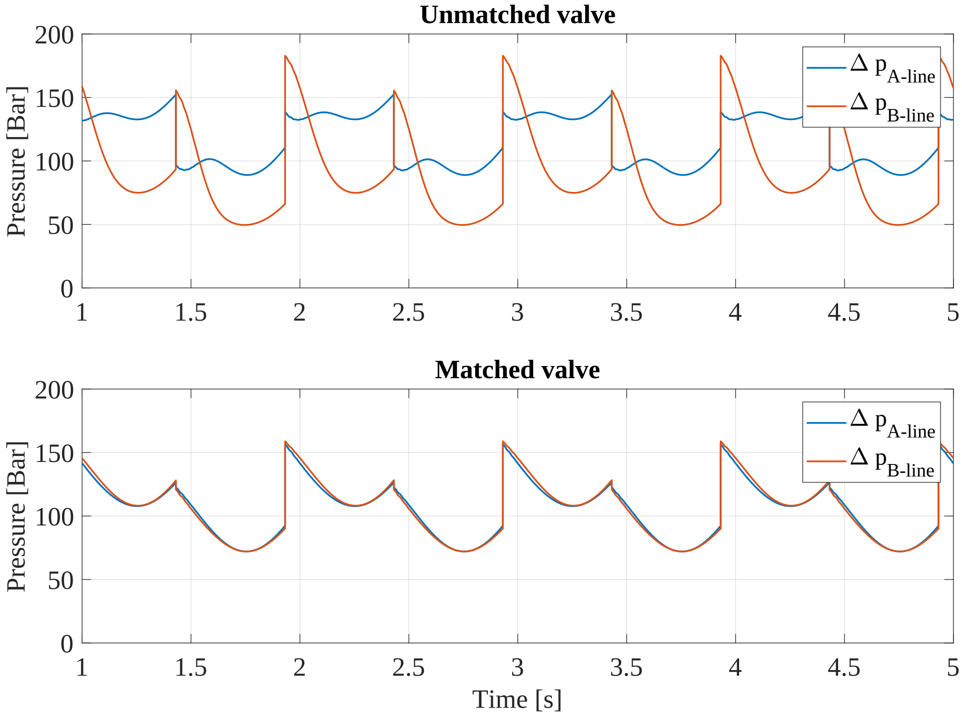

Figure 7.2. Comparison of pressure drop across the valve with an unmatched and a matched valve.

The chamber pressures are plotted in Figure 7.3 to investigate how they behave when employing the matched valve.

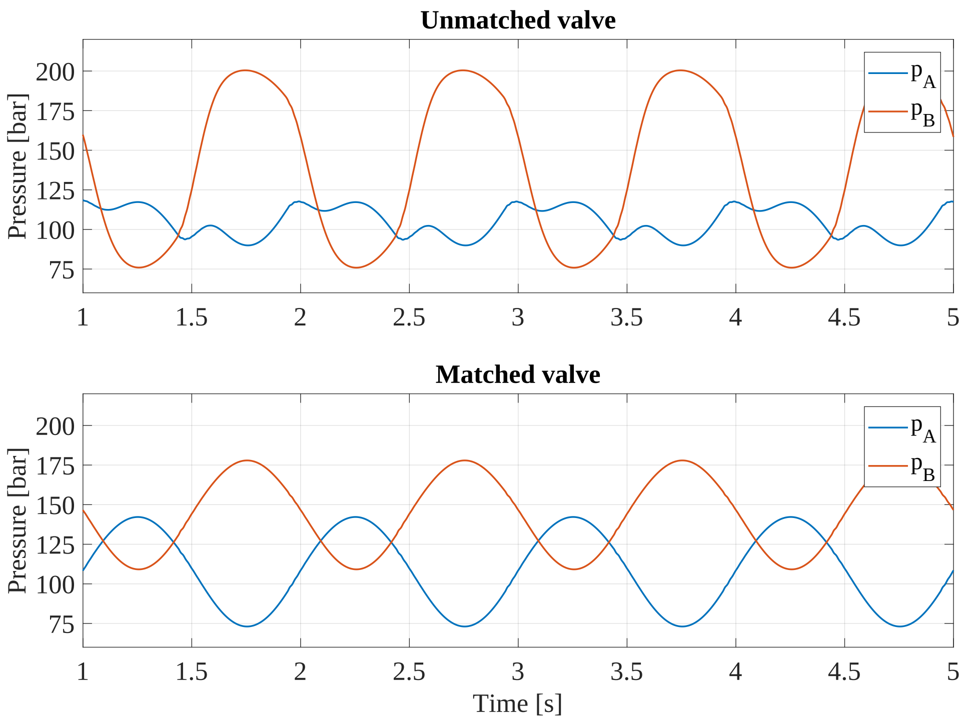

Figure 7.3. Comparison of chamber pressures with an unmatched and a matched valve.

For the system with the unmatched valve the piston side pressure is seen to have a magnitude ranging between 90 - 120 bar while the rod side pressure is seen to be varying more as it ranges between 75 - 200 bar. For the system with the matched valve both chamber pressures are seen to be sinusoidal both with an amplitude of 35 bar. Using the unmatched valve the minimum and maximum reached pressure levels are 75 and 200 bar, respectively. using the matched valve the minimum pressure reached is 75 bar as well but the maximum pressure reached is decreased to approximately 178 bar.

There is no indication that a superior force control is achieved when using either a matched valve or an unmatched valve. The chamber pressure levels are however acting smoother and the maximum pressure reached is decreased by 12 % indicating that a smaller supply pressure is needed when using a matched valve.

8 Force Control Design Considerations

When designing a force controller to a system, it should be determined which force in the system that should be controlled to achieve the desired force control. This force will often either be the load force which is defined as the force proportional to the load pressure, or it will be the resulting force which is the actual force applied by the cylinder. Which force that should be chosen depends on the application and the system. The most precise force control is achieved when controlling the resulting force as it accounts for friction forces in the cylinder. But in order to implement closed loop control, it is necessary to measure the resulting force which can be both expensive and even impossible at forces of great magnitude, as force transducers capable of measuring these forces are not available. In the test setup described in Chapter 2, both the pressures and the resulting force are measured, and for implementing force control in the system it seems reasonable to control the resulting force as it accounts for friction in the cylinder, and thereby yields the most precise control. The HALT test bench described in Chapter 1 has no force transducers for measuring the force. Instead cylinders with low friction ratings have been chosen so that the load force is seen as a reasonable approximation of the resulting force and may be used as feedback for the force control. In general, the most precise force control should be achieved when using the resulting force, but using the load force will probably be the most cost efficient solution and often yield satisfactory results anyway.

For the system described in Chapter 2, it was found that a P controller resulted in a stationary error on the force, and satisfactory force tracking performance around the linearisation point was achieved by implementing a PI controller. For the purpose of controlling the force at working points at or close to the linearisation point, it may be sufficient to implement a P or a PI controller dependent on the system.

When the working point was moved away from the linearisation point, the force was still tracking the reference but with a notable increase in the error. To improve the controller performance, a valve compensator was employed to cancel out the gain from the valve. The compensator using supply, tank and piston side chamber pressures was found to have better flow estimation compared to the compensator using supply, tank and both chamber pressures. Based upon this it is suggested to compensate using only the pressure in the chamber in which the flow in and out is controlled, in addition to supply and tank pressures. It is possible to implement the compensator in a system where it is not possible to measure the valve spool position as the valve signal may be used for governing the compensator. This may however only be done when the valve dynamic is sufficiently fast as otherwise a mismatch between the used pressure drop and the actual pressure drop will occur. The force reference may be used, but it should be performed carefully as a phase shift may be present between the force and the valve spool position, and it is recommended to use the force reference to govern the control only when neither the valve signal nor the valve spool position may be measured. For systems designed for operating at constant load forces resulting in approximately constant chamber pressures, it is concluded that an approximate of the mean pressure in the controlled chamber may be used as a constant pressure in the compensator. However the pressures will often be measured anyway for calculating the load pressure for the force control, and the actual chamber pressure may as well just be fed to the compensator. When implementing a compensator in systems with varying chamber pressure, it is suggested that the actual system pressures are fed to the compensator as it was found that feeding a constant supply pressure of much different magnitude than the actual pressure to the compensator resulted in amplification of oscillations and disturbances. It should be noted that both compensators were evaluated using constant supply and tank pressures. These may fluctuate in an actual operating system, and it is uncertain how this affects the performance of the two compensators.

When the system was modified by switching the symmetrical valve with a valve matched to the cylinder, satisfactory force tracking performance was achieved using the previously developed flow controller and the compensator using tank, supply and piston side pressure. The force tracking performance was approximately similar to that of the system with the symmetrical valve. No indication of a superior system design was found using either of the two valves. However lower peak pressures and smoother pressure gradients were found using a matched valve. It is worth noting that by employing a valve compensator the linear model used for designing the flow controller is independent of the valve flowpath ratio, and the designed flow controller may be employed in either system.

An aspect of force control using a compensator that has not been analysed in this report is to determine if the flow to be controlled should always be the flow into a chamber, the flow out of a chamber, or the flow in and out of a single chamber with the latter being the case for the compensation designed in this report. Such considerations are referred to as determining which metering-edge to govern the control. Controlling only the flow into a chamber or only the flow out of a chamber is referred to as controlling the meter-in or the meter-out, respectively, while the option used in this report is referred to as meter-in/meter-out as it is always the flow to the piston side chamber that is controlled independent of whether the flow is into or out of the chamber. Which metering-edge used for governing the control may influence the controller performance due to different dynamic for flow in and out and for flow to and from one chamber or to and from the other chamber. Furthermore it may be related to safety concerns regarding system operation. Imagine a vertically installed cylinder elevating a heavy load. If the flow into the rod side chamber is now controlled, it is not guaranteed that the piston side chamber will maintain a pressure sufficient for carrying the load, and the piston may drop and hit the end stop. In such a scenario it would be plausible to instead control the flow of the piston side chamber. This issue should be examined with respect to the system in question, and which metering-edge to govern the control should be considered for the reasons outlined.

9 Conclusion

A non linear model of the servo actuator system was derived, and the behaviour of the modelled system was compared to the behaviour of the actual system when the valve was given a step of 2 %. The simulated system dynamic was seen to be somewhat similar to that of the measured, but with a steady state error on the chamber pressures resulting in the simulated pressures being too low while the simulated piston movement was found to be slightly too slow in the positive direction and slightly too fast in the negative direction. It was proposed that this deviation was caused by an offset in the valve, and it was concluded that the non linear model sufficiently depicts the actual system for the purpose of designing and testing force controllers.

From the non linear model a linear model was derived and validated. Based on the linear model, a frequency response analysis of the system was conducted, and it was found that the valve dynamic should be included in the linear model when designing a force controller. A PI controller was designed and found to have satisfactory force tracking performance with a mean error of 1.3 kN when given a sinusoidal force reference with a frequency of 1 Hz and an amplitude of 30 kN. It was suggested that most of this error is caused by a small phase shift between the force and the reference as the system is struggling to keep up with the reference.

To improve the controller performance, a valve compensator was designed to cancel out the valve gain. Superior performance was seen when compensating with respect to the piston side chamber pressure only compared to compensating with respect to the load pressure as it had the better flow estimation and a marginally smaller error. A flow controller was designed based on a linear model with the reference flow as input. Using the flow controller and the compensator, the mean error was reduced by 146 % to 533 N compared to the original controller when given the same force reference. Using the pressures as feedback, the full controller had close to similar performance when reducing the supply pressure by 60 % as the mean error was seen to increase by 3 % to 550 N while the mean error for the original controller was seen to increase by 136 % to 3098 N. With fast valve dynamic relative to the respective system, it was found that the valve signal may be used for governing the compensator instead of the valve spool position. It is possible to have the force reference govern the compensator, but it should be performed carefully as it may cause discontinuities in the system response.

When changing the symmetrical valve for a matched valve, similar force tracking performance was achieved, and no indication of a superior force control was found using either of the two valves. Using the matched valve did however result in smoother pressure gradients in the cylinder chambers, and the needed supply pressure was reduced by 12 %.

10 Reflection

Further work on this project would be to implement the developed force controllers in the laboratory setup and investigate their performance. It would be interesting to see the PI controller performance and compare it to the controller performance when a valve compensator is employed. Furthermore it would be interesting to compare the performance of the compensator when compensating with respect to the piston side chamber pressure and the load pressure, respectively. Finally it would also be of interest to investigate the compensator performance when the valve signal is used to govern the compensator instead of the valve spool position.

It would be plausible to design a flow controller for controlling the valve flow to the rod side chamber as well. Using this controller and the one developed in the report for controlling the piston side flow, it would be possible to design a control structure that either solely controls flow into the system or solely controls flow out of the system. Subsequently it would be possible to investigate the characteristics of the two control approaches and compare the controller performance when the meter-in is governing the control to the controller performance when the meter-out is governing the control.

Bibliography

Andersson et al., 2005. Sören Andersson, Anders Söderberg og Stefan Björklund. *Friction models for sliding dry, boundary and mixed lubricated contacts*, Department of Machine Design, Machine Elements, Royal Institute of Technology, Stockholm, Sweden, 2005.

Hansen et al., 2016. Anders Hedegaard Hansen, Lasse Schmidt, Henrik C. Pedersen og Torben O. Andersen. *A GENERIC MODEL BASED TRACKING CONTROLLER FOR HYDRAULIC VALVE-CYLINDER DRIVES*, Department of Energy Technology, Aalborg University, 2016.

MOOG, 2009. MOOG. *DIRECT DRIVE SERVOVALVES D633/D634*. Datasheet, 2009.

System Parameters A

This Appendix contains parameter values for the system setup described in Chapter 2.

General system parameters

Variable	Description	Value	Unit
β	Bulk modulus	8000	bar
M_s	Sliding mass	700	kg
M_tot	Total moving mass	730	kg
p_S	Supply pressure	250	bar
p_T	tank pressure	1	bar

Table A.1. General system parameters.

Load cylinder parameters

Variable	Description	Value	Unit
A_A	Piston side area	0.005	m^2
A_B	Rod side area	0.0038	m^2
α	Area ratio	0.75	-
D	Piston diameter	80	mm
d	Rod diameter	40	mm
L	Stroke length	700	mm
M	Piston mass	20	kg

Table A.2. Load cylinder parameters.

Valve parameters

Variable	Description	Value	Unit
u_v	Valve signal	± 10	V
Δp_N	Nominal pressure drop	35	bar
Q_N	Nominal flow	100	l/min
k_s	Gain from opening area to voltage drop	0.1	m/V
ω_v	Natural frequency	377	rad/s
ζ_v	Damping	1	-
$\dot{x}_\mathrm{v,max}$	Slew rate limit	± 80	1/s

Table A.3. MOOG D634 valve parameters.